NASA CR- 72419

EIGHTH QUARTERLY REPORT

ELECTROCHEMICAL CHARACTERIZATION OF NONAQUEOUS SYSTEMS FOR SECONDARY BATTERY APPLICATION

February - April 1968

by

M. Shaw, O. A. Paez, D. A. Lufkin, A. H. Remanick

prepared for

NATIONAL AERONAUTICS AND SPACE ADMINISTRATION

May 17, 1968

CONTRACT NAS 3-8509

Technical Management
Space Power Systems Division
National Aeronautics and Space Administration
Lewis Research Center, Cleveland, Ohio
Mr. Robert B. King

NARMCO RESEARCH AND DEVELOPMENT DIVISION

OF

WHITTAKER CORPORATION
3540 Aero Court
San Diego, California 92123

TABLE OF CONTENTS

LIST OF TABLES

CYCLIC VOLTAMMOGRAMS

ELECTROCHEMICAL CHARACTERIZATION OF NONAQUEOUS SYSTEMS FOR SECONDARY BATTERY APPLICATION

by

M. Shaw, O. A. Paez, A. H. Remanick, D. A. Lufkin

ABSTRACT

Electrode compatibility tests on wire electrodes have been completed for the twenty-four selected positive systems. The charged state solubility has been determined for sixteen of these systems.

The screening of negative systems involving lithium, magnesium, and calcium has been completed during this reporting period.

SUMMARY

The electrochemical characterization of nonaqueous battery systems has now been completed. A list of twenty-four positive-electrolyte systems recommended from a total of 950 was presented in the preceding report (Ref. 1). Wet stand compatibility tests on wire electrodes have now been completed for the twenty-four systems, and the solubility of the charged state reactants (metal cation) have been determined for sixteen of these systems. The results indicate that solubility and reactivity are complicating factors whose effect on compatibility can vary with the nature of the electrode surface. The results, therefore, on smooth surface wire electrodes, may not accurately project wet stand compatibility of sintered metal plates. A new program for testing charge retention as a function of capacity, using porous electrodes, has therefore been scheduled.

The screening of negative systems involving lithium, magnesium, and calcium has been completed. Cyclic voltammograms were obtained for 64 such systems.

I. ELECTRODE COMPATIBILITY

Standard compatibility tests on 24 selected systems have now been completed. Solubility of the charged state reactants has been determined for 16 of these systems. Solubility and electrode surface nature are complicating factors, such that the standard compatibility test may not be effective as a screening device.

A. Standard Compatibility Test

Eighteen systems were subjected to the standard compatibility test (Ref. 1.) Since most systems suffered greater than 50% loss of discharge after 15 minutes stand time, an additional 5-minute stand time interval was measured in all cases. A minimum of three zero stand time measurements was recorded in all tests. The reproducibility of the zero stand time varied with the system, from a few percent to as much as 50% in some instances. Table I lists the average zero stand time capacity (mcoul/cm^2 delivered at 1 ma/cm^2 immediately after completion of the sweep charge), and the percent of zero stand time capacity retained after 5 and 15 minutes of stand.

Three systems, Cu/AN-$LiPF_6$ + KPF_6, Cd/DMF-$LiBF_4$, and Zn/DMF-$LiPF_6$, showed a continuous discharge even after replacement of the working electrode with a fresh metal electrode not previously charged. Since wet stand had no apparent effect, these results indicate reduction of some dissolved species. The discharge potential was comparable to that obtained for discharge of electrode active material, indicating the dissolved species might have been obtained from the electrode. Further confirmation is necessary.

The system, AgO/BL-LiCl + $AlCl_3$, exhibited instrument overload during sweep charging, so was charged and discharged under a constant current of 4 ma/cm^2. Compared to the other systems charged by a sweep mode, capacity retention for the silver electrode was considerably greater

TABLE I

CAPACITY RETENTION AFTER 5
AND 15 MINUTES OF STAND TIME*

System	Zero Stand Time Capacity	% Retention After 5 min	% Retention After 15 min
	Millicoul/cm^2	%	%
$CuCl_2$/AN-$LiPF_6$	48	0	0
$CuCl_2$/BL-$AlCl_3$	212	9	0
$CuCl_2$/DMF-LiCl + $LiClO_4$	75	0	0
$CuCl_2$/DMF-$LiPF_6$	166	13	0
$CuCl_2$/PC-$LiClO_4$	653	55	23
CuF_2/DMF-$LiPF_6$	65	9	9
CuF_2/PC-$LiPF_6$	123	7	0
CuF_2/PC-$LiClO_4$	103	0	0
Zn/AN-$LiClO_4$	78	0	0
Zn/BL-KPF_6	144	0	0
ZnF_2/DMF-$LiClO_4$	77	0	0
ZnF_2/DMF-KPF_6	62	0	0
Cd/BL-KPF_6	165	25	4
Cd/DMF-KPF_6	522	37	9

* Electrodes charged by anodic sweep and discharged galvanostatically at 1 ma/cm^2.

AN - Acetonitrile
BL - Butyrolactone
DMF - Dimethylformamide
PC - Propylene carbonate

(70% after 1 hour of stand time). Even greater retentivity was obtained as a result of sweep cycling the electrode. This is shown in Table II. A fresh silver electrode, placed in the electrolyte at the conclusion of these measurements, indicated no reduction of species in solution at 4 ma/cm^2 within -1.0 v relative to a silver oxide reference. The capacity retention of this system is comparable to that of the aqueous silver oxide system reported previously (Ref. 1.)

B. Solubility of Charged State Material

As reported earlier (Ref. 1), measurements, in solutions saturated with the charged state material, did not show any improvement in apparent capacity retention, which would be expected if capacity loss was due to electrode solubility. To evaluate this further, solubility measurements were made for 16 systems.

Saturated solutions were prepared by potentiostatic oxidation of wire electrodes, relative to metal/metal halide reference electrodes where the metal was common to the working electrode. (Reference electrodes were prepared in-situ by electrooxidation at 1 ma/cm^2 for 1 or 2 minutes to insure a steady reference voltage). In charging the working electrode, the potential was applied gradually until a steady limiting current was reached. This potential was generally between +0.3 v to +0.5 v, relative to the reference electrode. Pre-halogenated electrodes were discharged at -0.3 to -0.5 v for 15 to 20 minutes prior to charging. The working electrodes were made from 50 mil diameter wire with 1-inch exposed to the electrolyte (initial area = 1 cm^2). Electrolyte volume was 25 ml.

Potentiostatic charging of the electrodes was continued until significant visual evidence of precipitation was indicated. The total coulombs

TABLE II

CAPACITY RETENTION OF AgO/BL-LiCl + $AlCl_3$
AFTER 1 AND 24 HOURS OF STAND TIME*

	Charge coul/cm^2	Zero Time %	Percent Retention After 5 min %	15 min %	1 hour %	24 hours %
a)	(No pretreatment)					
	0.96	-	-	-	64	-
	2.40	72	-	-	70	0
b)	(Activated by sweep cycling)					
	0.96	110**	97	106**	-	-
	2.93	-	-	-	93	-
	2.54	-	-	-	-	43

* Charged and discharged at 4 ma/cm^2 constant current.

** Retention of greater than 100% may reflect oxidation products remaining from the sweep cycling phase.

passed during the charging period were calculated from the current-time curve. After charging, the electrolyte was removed from the cell and filtered. A 1-ml aliquot was then taken, diluted to a known volume of aqueous electrolyte, and analyzed by DME polarography. Aqueous electrolytes of 0.1 M KCl, 1 M KCl, and 1 M HCl were used for analysis of zinc, cadmium, and copper unknowns respectively. The method of standard addition was used to determine concentration. A Sargent Polarograph model XV was used in these analyses.

Results are tabulated in Table III, showing the total number of coulombs passed during the charge process, and the metal ion concentration in solution. Also given are the equivalent coulombs of material in solution. Comparing these values with the total coulombs passed, shows that all solutions were saturated.

In those cases where data are available for systems having a common cathode and electrolyte salt, there is a relationship between charged state material solubility and delivered capacity at zero stand time. Table IV shows this for Zn/KPF_6 and $CuF_2/LiPF_6$, indicating that the delivered capacity increases with decreasing metal ion solubility. Comparison of the entire list, however, shows several inconsistencies. $CuCl_2/PC\text{-}LiClO_4$ shows the second lowest solubility and the largest delivered capacity at zero stand time (Table I). Accordingly, it also shows the greatest retentivity after 5-minutes stand time. On the other hand, $Cd/DMF\text{-}KPF_6$ compares well with $CuCl_2/PC\text{-}LiClO_4$ in terms of capacity retention at zero and 5-minutes stand time, yet it has the second highest solubility. Again, even though continuous discharge is found with systems having solubilities in excess of 17 mmoles/liter, other systems having as high a solubility, exhibit limited discharge times related to capacity retention.

TABLE III

SOLUBILITY OF CHARGED STATE MATERIAL*

System	Cation Concent. mmoles/liter	Coulombs** Dissolved coulombs	Total Charge coulombs
ZnF_2/DMF-KPF_6	1.96	10	236
$CuCl_2$/PC-$LiClO_4$	2.19	11	191
CuF_2/PC-$LiPF_6$	2.61	13	127
Zn/DMF-KPF_6 (2.0 m)	3.70	18	331
Zn/DMF-KPF_6 (0.75 m)	4.40	21	324
CuF_2/DMF-$LiPF_6$	5.28	25	138
Cd/DMF-$LiClO_4$	6.30	30	338
Zn/BL-KPF_6	10.8	52	146
Zn/PC-KPF_6	13.4	65	125
Cu/DMF-$LiPF_6$	14.4	58	158
Zn/DMF-$LiPF_6$ (a)	17.9	86	740
$CuCl_2$/AN-$LiPF_6$	29.7	91	449
Cu/AN-$LiPF_6$ + KPF_6 (a)	33.0	100	224
$CuCl_2$/BL-$AlCl_3$	35.0	107	108
Cd/DMF-KPF_6	37.6	181	302
Cd/DMF-$LiBF_4$ (a)	40.2	193	562

* Arranged in order of increasing solubility.

** Electron stoichiometry for copper systems based on polarographic wave heights for Cu(I) and Cu(II); a two electron change is assumed for zinc and cadmium.

(a) These systems showed a continuous discharge independent of stand time, possibly representing discharge of dissolved species.

AN - Acetonitrile
BL - Butyrolactone
DMF - Dimethylformamide
PC - Propylene carbonate

TABLE IV

EFFECT OF SOLUBILITY OF CHARGED STATE MATERIAL ON ZERO STAND TIME CAPACITY

System	Cation Concent. mmoles/liter	Zero Stand* Time Capacity mcoul/cm^2
Zn/DMF-KPF_6 (2.0 m)	3.7	256
Zn/DMF-KPF_6 (0.75 m)	4.4	205
Zn/BL-KPF_6	10.8	144
Zn/PC-KPF_6	13.4	106
CuF_2/PC-$LiPF_6$	2.61	123
CuF_2/DMF-$LiPF_6$	5.28	65

* Discharge at 1 ma/cm^2 immediately following sweep charging.

BL - Butyrolactone
DMF - Dimethylformamide
PC - Propylene carbonate

The results obtained on the "compatibility" of wire electrodes make it evident that the concentration of the charged state material in the electrolyte, as well as the surface nature of the electrode, and the charge density of the formed material, are influencing factors. In some cases, electrode pretreatment, such as by continued sweep cycling, affects the results. The standard compatibility test involved sweep charge and constant current discharge. Sweep charge does not permit a constant coulombic input for all systems, and the preliminary ten cycles of sweep charge and discharge introduced a varying amount of material into the solution. This has made it impossible to evaluate the data on a comparable basis.

Further screening of the recommended systems must consider these factors, as well as the vital necessity of distinguishing reduction of solid state charged material from that of dissolved state charged material.

II. CYCLIC VOLTAMMETRY

A. Analysis of Cyclic Voltammograms

The characterization of nonaqueous systems involving lithium, magnesium, and calcium negatives by cyclic voltammetry has been completed during this reporting period. A total of 64 systems have been screened to date. These are listed in Tables V and VI. Table VII lists the conductivities of the solutions screened. As before, the cyclic voltammograms are represented with the anodic reaction above the voltage axis, and the cathodic reaction below this axis. Since these are reactions involving the negative plate, however, the anodic reaction now represents the discharge reaction, and the cathodic, the charge reaction.

1. Systems Involving Chloride and Perchlorate Electrolytes

Lithium appears to have a lower activity in LiCl than in $LiClO_4$ and $AlCl_3$ solutions. Calcium electrodes show generally greater activity in LiCl and $AlCl_3$ solutions and are least active in $LiClO_4$ solution. No solute effect is evident for magnesium. Magnesium and calcium electrodes are most active in acetonitrile solutions. (Lithium was not screened in acetonitrile).

a. Lithium Electrode

(1) Butrolactone solutions

The cyclic voltammogram for lithium in $LiClO_4$ solution is shown in Figure 1 (CV-4135). The curve shows broad polarized anodic and cathodic peaks in the high current density range with more than 1.5 v between peaks. A similar curve results for lithium in $AlCl_3$ solution. Low anodic and medium high cathodic peaks result for LiCl + $AlCl_3$ solutions as shown in Figure 2 (CV-4147).

TABLE V

ELECTROCHEMICAL SYSTEMS SCREENED
CHLORIDE AND PERCHLORATE ELECTROLYTES

Solvent / Solute	Acetonitrile	Butyrolactone	Dimethylformamide	Propylene carbonate
LiCl			Li, Mg, Ca	
$LiClO_4$	Mg, Ca	Li, Mg, Ca	Li, Mg, Ca	Li, Mg, Ca
$LiCl + LiClO_4$			Li, Mg, Ca	
$AlCl_3$	Mg, Ca	Li, Mg, Ca		
$LiCl + AlCl_3$	Mg, Ca	Mg, Ca, Li		Li, Mg, Ca
$MgCl_2$			Mg	Li, Mg
$Mg(ClO_4)_2$	Mg		Mg	Li

TABLE VI

ELECTROCHEMICAL SYSTEMS SCREENED
FLUORIDE ELECTROLYTES

Solvent / Solute	Acetonitrile	Butyrolactone	Dimethylformamide	Propylene carbonate
$LiPF_6$	Mg, Ca		Li, Mg, Ca	Li, Mg, Ca
KPF_6	Mg,	Li, Mg, Ca	Li, Mg, Ca	Li, Mg, Ca
$LiBF_4$	Mg, Ca		Li, Mg, Ca	Mg, Ca, Li
$LiPF_6 + KPF_6$	Mg, Ca			

TABLE VII

ELECTROLYTE CONDUCTIVITY *

Electrolyte	Molality m	Conductivity $ohm^{-1} cm^{-1}$
Acetonitrile-$AlCl_3$	1.0	4.5×10^{-2}
Acetonitrile-KPF_6 + $LiPF_6$	0.5 (a)	4.3×10^{-2}
Acetonitrile-KPF_6	0.75	3.3×10^{-2}
Acetonitrile-$Mg(ClO_4)_2$	1.0	3.3×10^{-2}
Acetonitrile-$LiClO_4$	0.75	3.0×10^{-2}
Dimethylformamide-$LiClO_4$	0.5	2.6×10^{-2}
Dimethylformamide-KPF_6	0.75	2.1×10^{-2}
Dimethylformamide-$Mg(ClO_4)_2$	0.75	1.9×10^{-2}
Acetonitrile-$LiPF_6$	0.5	1.7×10^{-2}
Acetonitrile-$AlCl_3$ + LiCl	0.25 (a)	1.5×10^{-2}
Dimethylformamide-LiCl + $LiClO_4$	0.75 (a)	1.4×10^{-2}
Butyrolactone-$AlCl_3$ + LiCl	0.5 (a)	1.1×10^{-2}
Butyrolactone-$AlCl_3$	0.5	1.0×10^{-2}
Butyrolactone-$LiClO_4$	1.0	1.1×10^{-2}
Dimethylformamide-$LiPF_6$	0.5	9.0×10^{-3}
Dimethylformamide-$MgCl_2$	0.5	8.4×10^{-3}
Dimethylformamide-LiCl	0.5	7.7×10^{-3}
Dimethylformamide-$LiBF_4$	0.5	7.3×10^{-3}
Butyrolactone-KPF_6	0.75	7.1×10^{-3}
Propylene carbonate-$LiClO_4$	1.0	5.8×10^{-3}
Propylene carbonate-$LiPF_6$	0.5	5.7×10^{-3}
Propylene carbonate-$AlCl_3$ + LiCl	0.5 (a)	5.3×10^{-3}
Propylene carbonate-KPF_6	0.75	4.5×10^{-3}
Propylene carbonate-$LiBF_4$	0.5	2.9×10^{-3}

* In order of decreasing conductivity.

(a) Concentration with respect to each salt.

(2) Dimethylformamide solutions

The cyclic voltammogram for lithium in $LiClO_4$ solution shows a broad, high anodic peak and a broad, low cathodic peak, whose sweep rate dependence indicates that soluble reactants are involved. In LiCl solution, lithium electrodes indicate very low anodic and cathodic activity. Results for the mixture LiCl + $LiClO_4$ are intermediate between that of the separate salt systems, showing low anodic and very low cathodic activity.

(3) Propylene carbonate solutions

Lithium in LiCl + $AlCl_3$ solution shows a broad, medium low range anodic peak. The cathodic sweep shows a broad, low range peak followed by erratic current behaviour at the negative voltage range. Lithium in $LiClO_4$ solutions shows very high anodic activity as evidenced by rapid dissolution and disintegration of the working electrode. However, this did not occur when the current was limited by switching periodically to open circuit during the anodic sweep. In this case the current was very high initially but fell off with additional cycling. The curve obtained after ten cycles shows broad, medium low anodic and cathodic peaks. In $MgCl_2$ solution, lithium shows broad, medium low anodic and cathodic peaks. The sweep curve is shown in Figure 3 (CV-4152). In $Mg(ClO_4)_2$, lithium shows broad, anodic activity with no peak formation and with maximum current in the low range. A broad asymmetric cathodic peak of low current range occurs near the open circuit voltage. The curve is shown in Figure 4 (CV-4197).

b. Magnesium Electrode

(1) Acetonitrile solutions

Magnesium electrodes in $LiClO_4$ solution show very high anodic activity but no cathodic activity. Anodic dissolution is evidenced by a decrease of the working electrode diameter to 1/3 of its original size. Similar results were noted for $Mg(ClO_4)_2$, $AlCl_3$, and LiCl + $AlCl_3$ solutions.

(2) Butyrolactone solutions

High anodic and no cathodic activity results for magnesium in LiCl + $AlCl_3$ and $AlCl_3$ solutions. A typical curve is shown in Figure 5 (CV-4023). A similar curve but with a medium low anodic peak results in $LiClO_4$ solution.

(3) Dimethylformamide solutions

High anodic and no cathodic activity similar to that in the preceding solvents results in LiCl, $LiClO_4$, $MgCl_2$, and $Mg(ClO_4)_2$ solutions. The similar occurs for LiCl + $LiClO_4$ mixture, except that a medium high anodic peak is observed.

(4) Propylene carbonate solutions

Magnesium exhibits a sharp high anodic peak in LiCl + $AlCl_3$ solution but again no cathodic activity is indicated. Very low anodic and cathodic activity results in $LiClO_4$ and $MgCl_2$ solutions.

c. Calcium Electrode

(1) Acetonitrile solutions

Very high anodic activity and some evidence of gassing is observed for calcium electrodes in LiCl + $AlCl_3$ solution. Medium low anodic activity is noted at the extreme negative potential range. High anodic activity accompanied by pronounced gassing results in $AlCl_3$ solution. The calcium electrode diameter was reduced to half its original size. Calcium electrodes in $LiClO_4$ solution result in a low anodic peak with no indications of cathodic activity.

(2) Butyrolactone solutions

Calcium electrodes in LiCl + $AlCl_3$ and in $AlCl_3$ solutions show a medium low anodic peak and very low cathodic activity. In $LiClO_4$ solutions, calcium shows very low anodic and cathodic activity. The curve in $AlCl_3$ solution is shown in Figure 6 (CV-3982).

(3) Dimethylformamide solutions

The curve for calcium in LiCl solution is shown in Figure 7 (CV-4053). Anodic activity occurs over a broad range with a sharp peak of medium high current density at the extreme positive range. Anodic current occurs at more negative potentials but only on the reverse sweep. This behavior is indicative of an activation process such as the formation of a surface reactant. Negligible cathodic activity is indicated.

Calcium electrodes in $LiClO_4$ solution show very low anodic and cathodic activity. The mixture of LiCl + $LiClO_4$ shows medium high anodic and very low cathodic activity. An anodic peak reoccurs on the reverse sweep. The sweep curve is shown in Figure 8 (CV-4012).

(4) Propylene carbonate solution

A broad, very low anodic peak and no cathodic activity results for calcium electrodes in $LiClO_4$ solution. No anodic or cathodic activity is observed for calcium in $AlCl_3$ + LiCl solutions.

2. Systems Involving Fluoride Electrolytes

Lithium electrodes show a trend toward higher anodic and cathodic electrochemical activity in $LiPF_6$ and $LiBF_4$ solutions over that observed in KPF_6 solutions. Magnesium and calcium electrodes tend toward higher anodic activity in acetonitrile solutions, and decreased activity in propylene carbonate and butyrolactone solutions.

a. Lithium Electrode

(1) Butyrolactone solution

Lithium electrodes in KPF_6 solution shows a high anodic peak and low cathodic activity. The curve is shown in Figure 9 (CV-4227).

(2) Dimethylformamide solutions

The cyclic voltammogram for lithium in $LiPF_6$ solution shows high, irreproducible anodic and cathodic activity with more than 1 volt separation between peaks. In KPF_6 solution, lithium electrodes show medium high anodic and low cathodic activity. Lithium in $LiBF_4$ solutions shows a broad, very high current anodic peak and medium high cathodic activity with poor reproducibility.

(3) Propylene carbonate solutions

Lithium electrodes in $LiPF_6$ solutions result in voltage overload at very high anodic and cathodic current densities while only low highly polarized anodic and cathodic activity results in KPF_6 solution. In $LiBF_4$ solution, lithium shows broad, high anodic and cathodic peaks accompanied by a darkening of the solution. The curve is shown in Figure 10 (CV-4097).

b. Magnesium electrodes

(1) Acetonitrile solutions

Magnesium electrodes show high anodic activity in $LiPF_6$, KPF_6, and $LiPF_6 + KPF_6$ solutions, but no cathodic activity. In all cases the magnesium working electrode diameter decreased during the measurements and in one case actually fell off, presumable due to rapid anodic dissolution. No peak formation results for magnesium in $LiPF_4$ solutions. Anodic and cathodic currents fall in the low and medium low range respectively.

(2) Butyrolactone solutions

Magnesium electrodes in KPF_6 solution show very low anodic and cathodic activity.

(3) Dimethylformamide solutions

Magnesium electrodes in $LiBF_4$, $LiPF_6$, and KPF_6 show respectively high, medium high and medium low anodic peaks. Medium low cathodic activity

at the negative potentials occurs in $LiBF_4$ and $LiPF_6$ solutions. No cathodic activity is observed in KPF_6 solutions. The curve in $LiBF_4$ solution is shown in Figure 11 (CV-4018).

(4) Propylene carbonate solutions

Magnesium electrodes in $LiPF_6$ and $LiBF_4$ solutions show broad, low current density anodic peaks and very low cathodic activity. No peak formation and only very low anodic and cathodic activity results in KPF_6 solution.

c. Calcium electrodes

(1) Acetonitrile solutions

Calcium electrodes in $LiPF_6$ and in $LiPF_6 + KPF_6$ solutions show a broad, high anodic peak and medium low cathodic activity with more than 1.5 v separation. Calcium in $LiBF_4$ solution shows very low anodic and cathodic activity and no peak formation.

(2) Butyrolactone solutions

Very low anodic and cathodic activity results for calcium electrodes in KPF_6 solution.

(3) Dimethylformamide solutions

The sweep curve for calcium in KPF_6 solution shows a single broad, activation polarized peak of medium high current density and low cathodic activity. A similar curve, shown in Figure 12 (CV-3992), results for calcium in $LiPF_6$ solution with anodic and cathodic current densities in the low and very low range, respectively. Similar results occur in $LIBF_4$ solution except that the anodic current does not peak out but continues to rise to the end of the anodic sweep.

(4) Propylene carbonate solutions

Calcium electrodes in $LiPF_6$ solution show low multipeak anodic activity. Low cathodic activity is indicated at the extreme negative end of the sweep. Broad, ill-defined, low anodic activity is observed in KPF_6 solution with cathodic activity in the very low range. Calcium in $LiBF_4$ solutions shows a broad, medium low anodic peak and high cathodic activity with no peak formation. The cathodic activity is likely to involve lithium ion from the electrolyte solution.

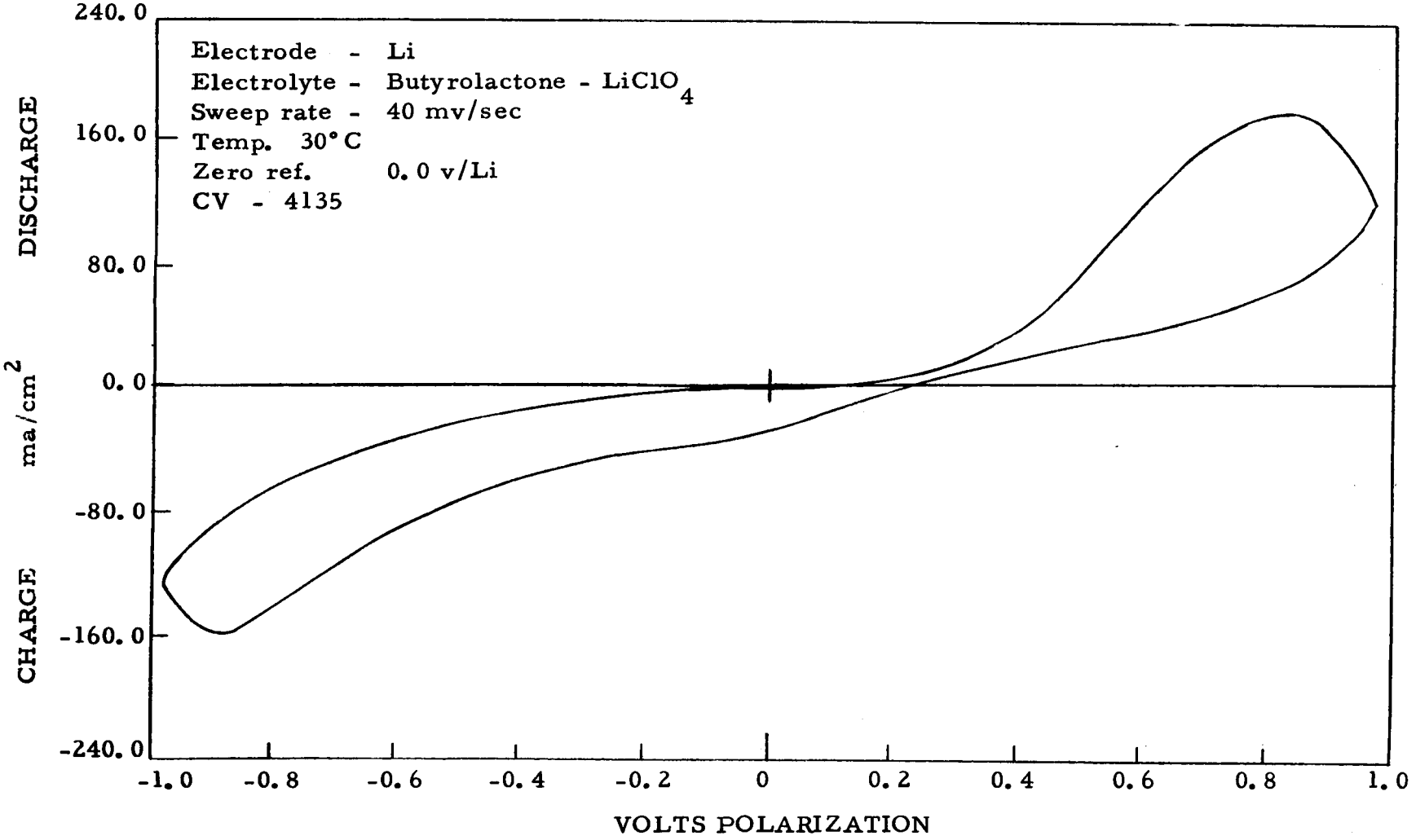
Electrode - Li
Electrolyte - Butyrolactone - $LiClO_4$
Sweep rate - 40 mv/sec
Temp. 30° C
Zero ref. 0.0 v/Li
CV - 4135
DISCHARGE
CHARGE
ma/cm^2
240.0
160.0
80.0
0.0
-80.0
-160.0
-240.0
-1.0
-0.8
-0.6
-0.4
-0.2
0
0.2
0.4
0.6
0.8
1.0
VOLTS POLARIZATION

Figure 1

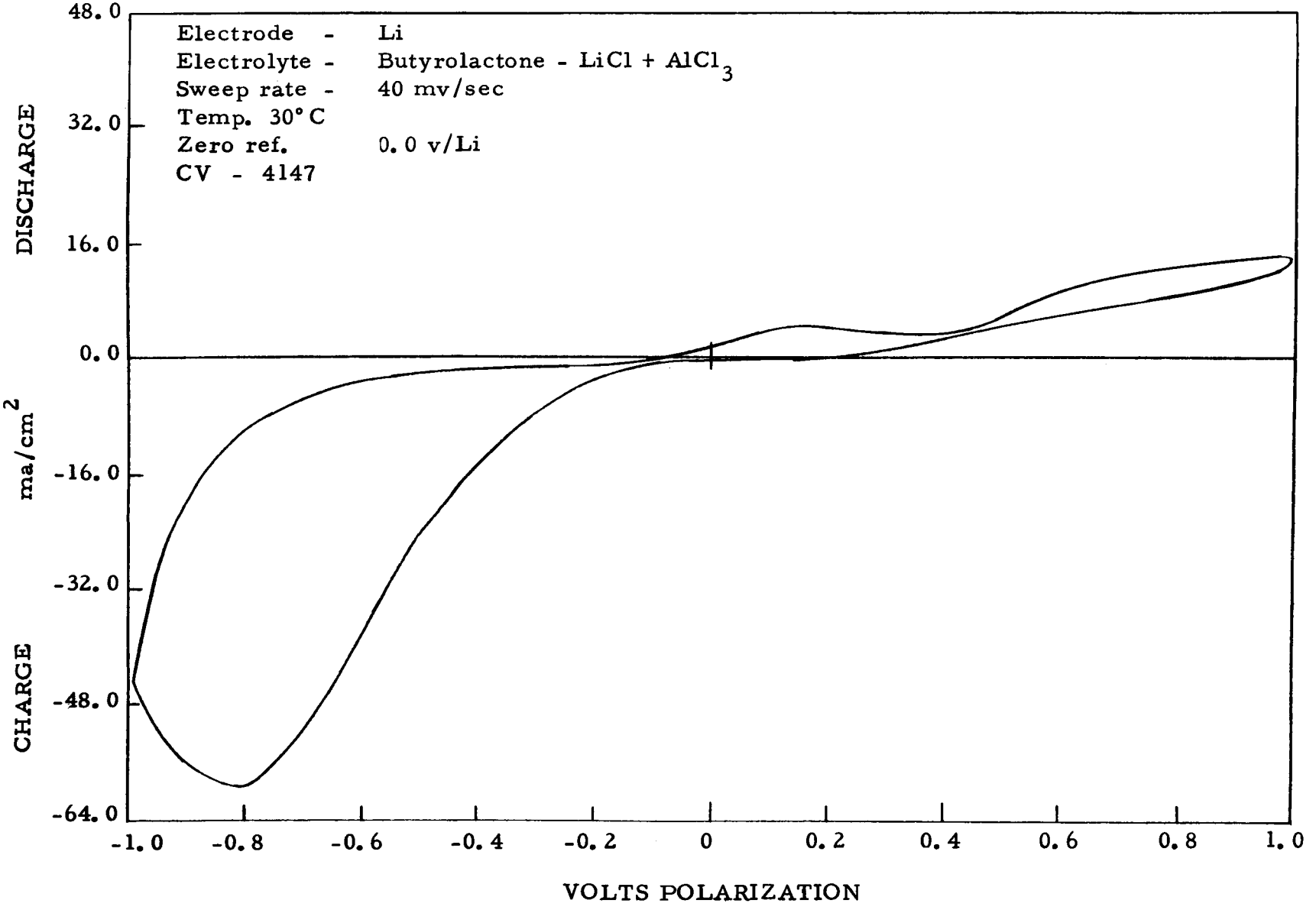
Electrode - Li
Electrolyte - Butyrolactone - LiCl + AlCl3
Sweep rate - 40 mv/sec
Temp. 30° C
Zero ref. 0.0 v/Li
CV - 4147
DISCHARGE
CHARGE
ma/cm2
48.0
32.0
16.0
0.0
-16.0
-32.0
-48.0
-64.0
-1.0
-0.8
-0.6
-0.4
-0.2
0
0.2
0.4
0.6
0.8
1.0
VOLTS POLARIZATION

Figure 2

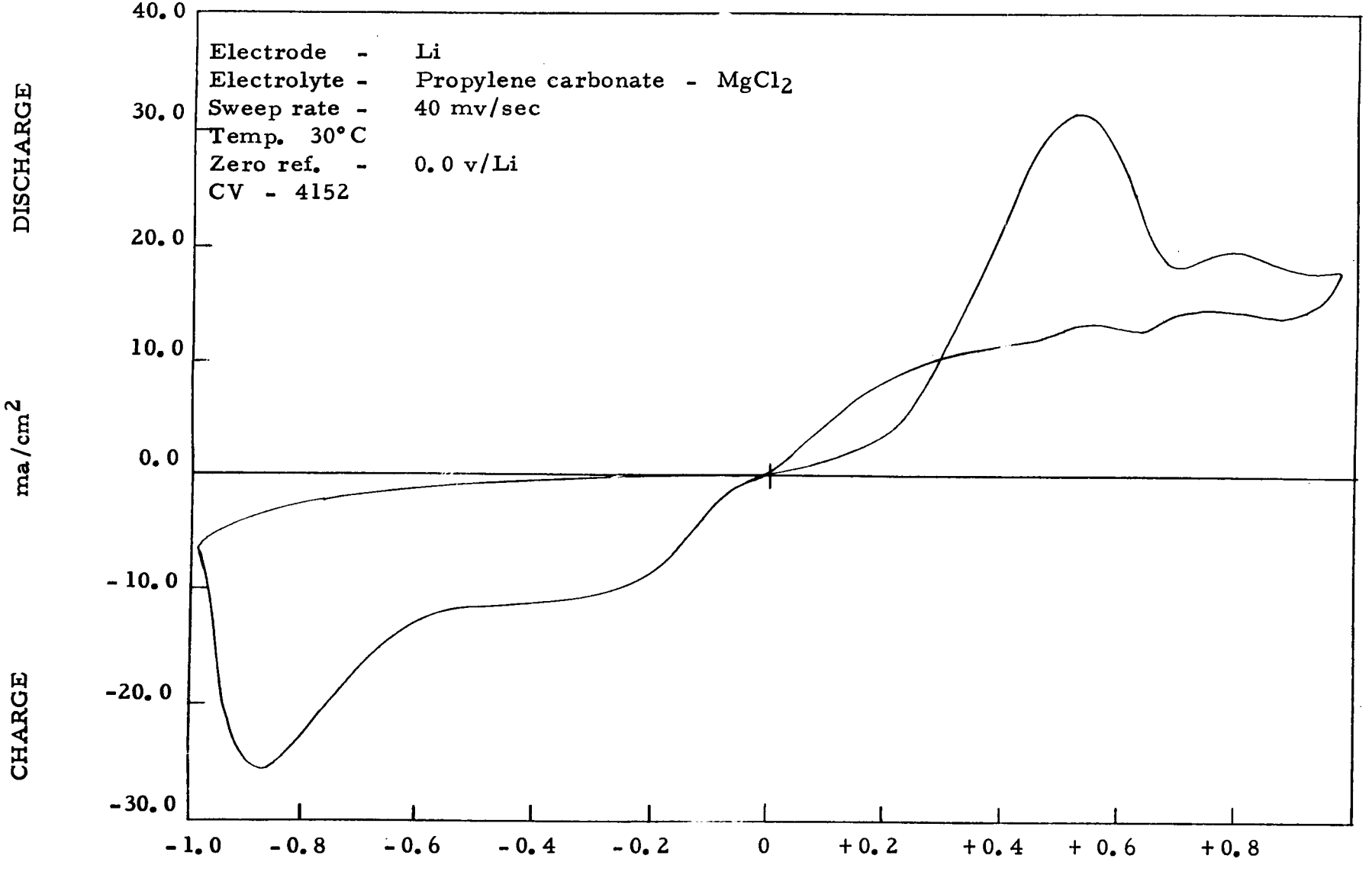
Electrode - Li
Electrolyte - Propylene carbonate - $MgCl_2$
Sweep rate - 40 mv/sec
Temp. 30°C
Zero ref. - 0.0 v/Li
CV - 4152
DISCHARGE
CHARGE
ma/cm²
40.0
30.0
20.0
10.0
0.0
-10.0
-20.0
-30.0
-1.0
-0.8
-0.6
-0.4
-0.2
0
+0.2
+0.4
+0.6
+0.8
VOLTS POLARIZATION

Figure 3

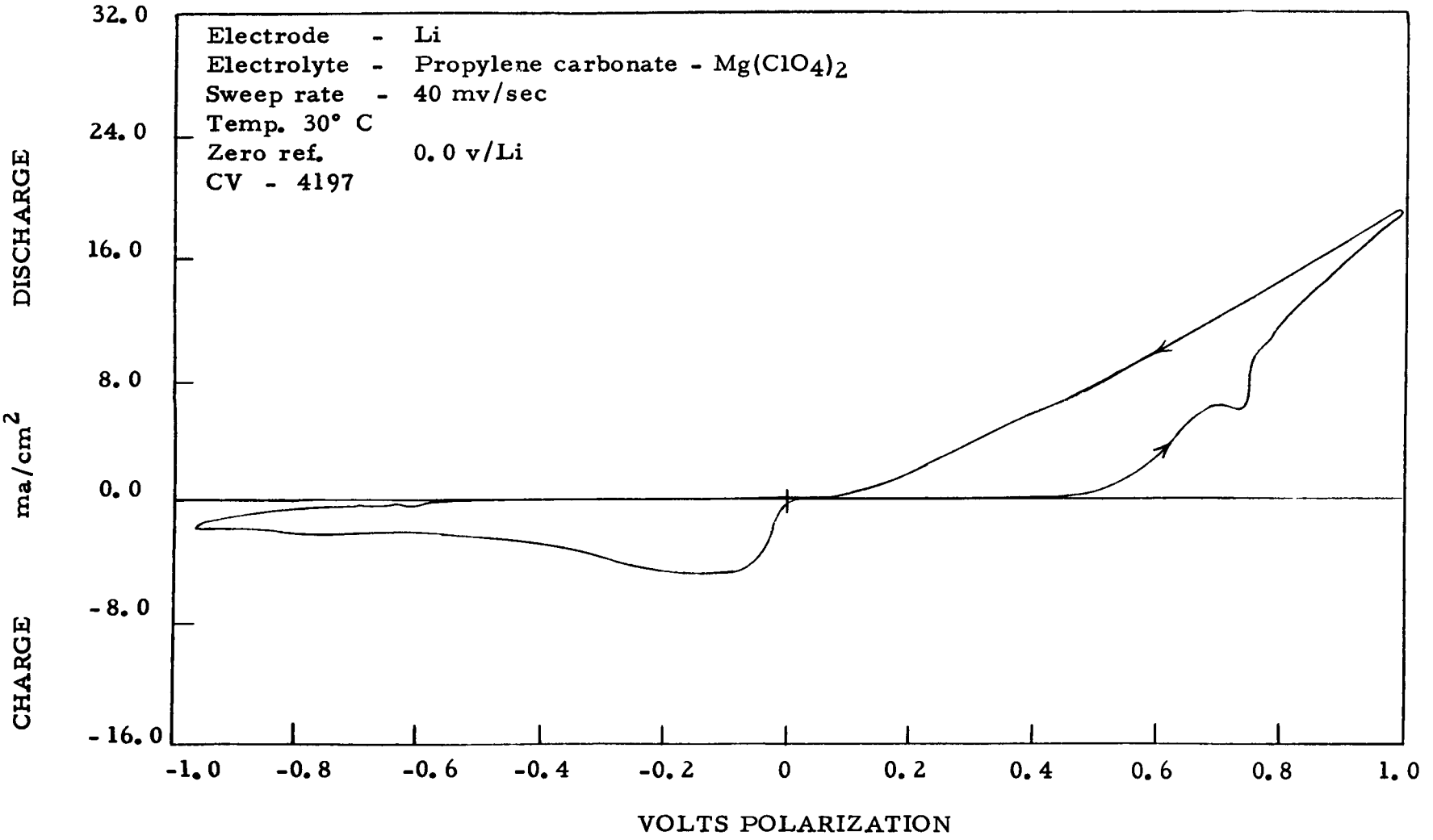
Electrode - Li
Electrolyte - Propylene carbonate - $Mg(ClO_4)_2$
Sweep rate - 40 mv/sec
Temp. 30° C
Zero ref. 0.0 v/Li
CV - 4197
32.0
24.0
16.0
8.0
0.0
-8.0
-16.0
DISCHARGE
CHARGE
ma/cm^2
-1.0
-0.8
-0.6
-0.4
-0.2
0
0.2
0.4
0.6
0.8
1.0
VOLTS POLARIZATION

Figure 4

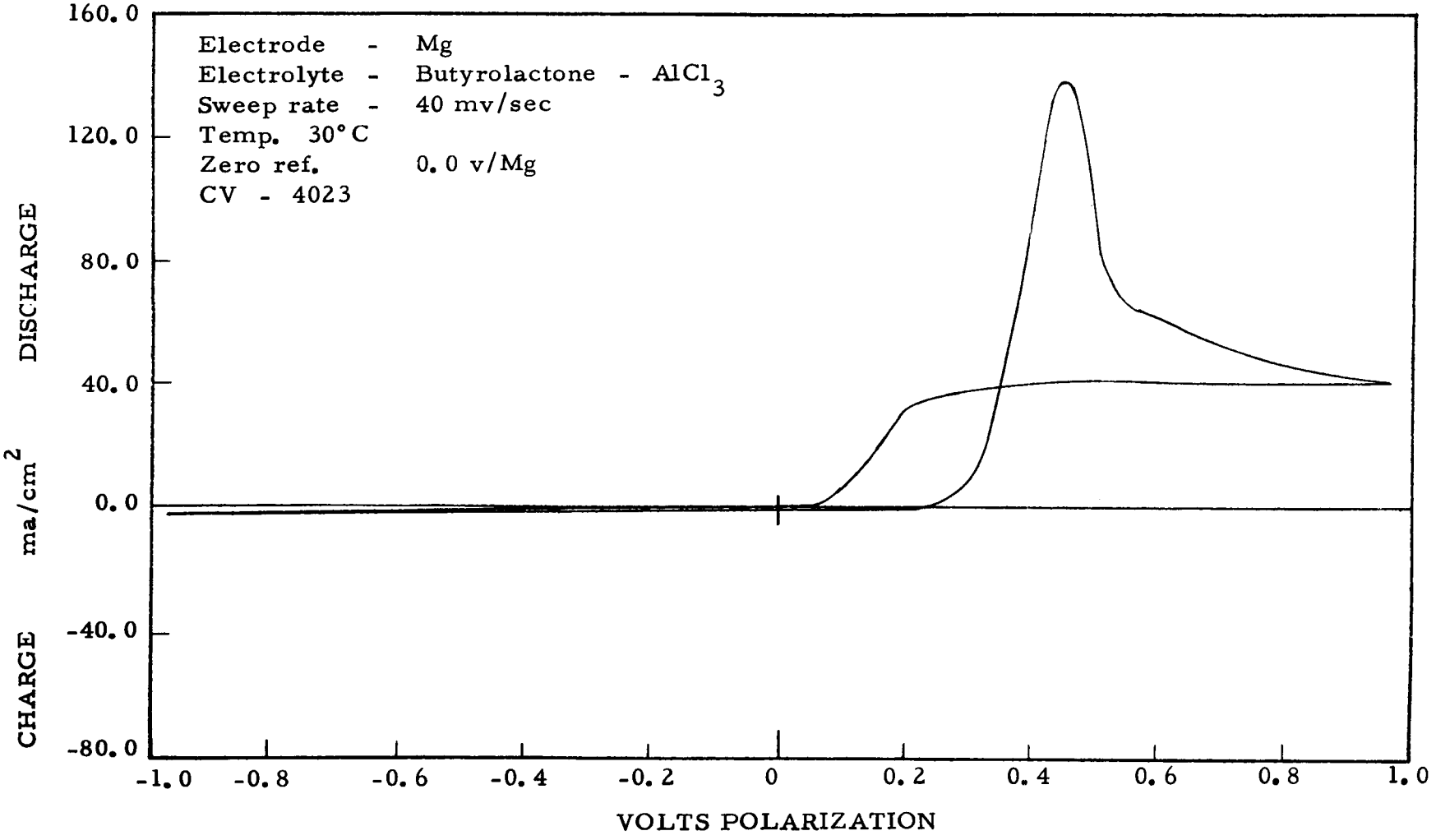
Electrode - Mg
Electrolyte - Butyrolactone - $AlCl_3$
Sweep rate - 40 mv/sec
Temp. 30°C
Zero ref. 0.0 v/Mg
CV - 4023
160.0
120.0
80.0
40.0
0.0
-40.0
-80.0
DISCHARGE
CHARGE
ma/cm^2
-1.0
-0.8
-0.6
-0.4
-0.2
0
0.2
0.4
0.6
0.8
1.0
VOLTS POLARIZATION

Figure 5

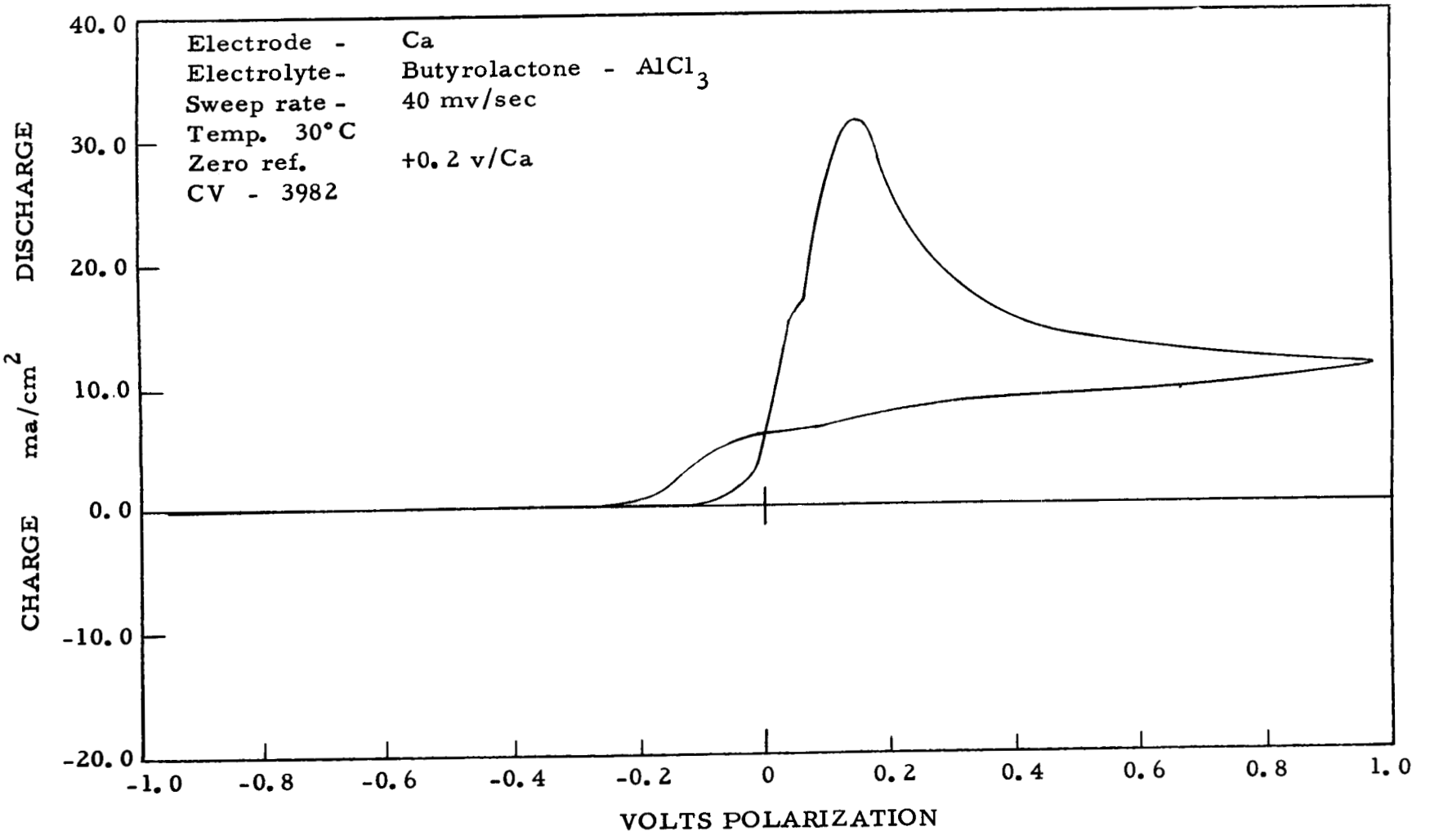
Electrode - Ca
Electrolyte - Butyrolactone - $AlCl_3$
Sweep rate - 40 mv/sec
Temp. 30° C
Zero ref. +0.2 v/Ca
CV - 3982
40.0
30.0
20.0
10.0
0.0
-10.0
-20.0
CHARGE ma/cm^2 DISCHARGE
-1.0
-0.8
-0.6
-0.4
-0.2
0
0.2
0.4
0.6
0.8
1.0
VOLTS POLARIZATION

Figure 6

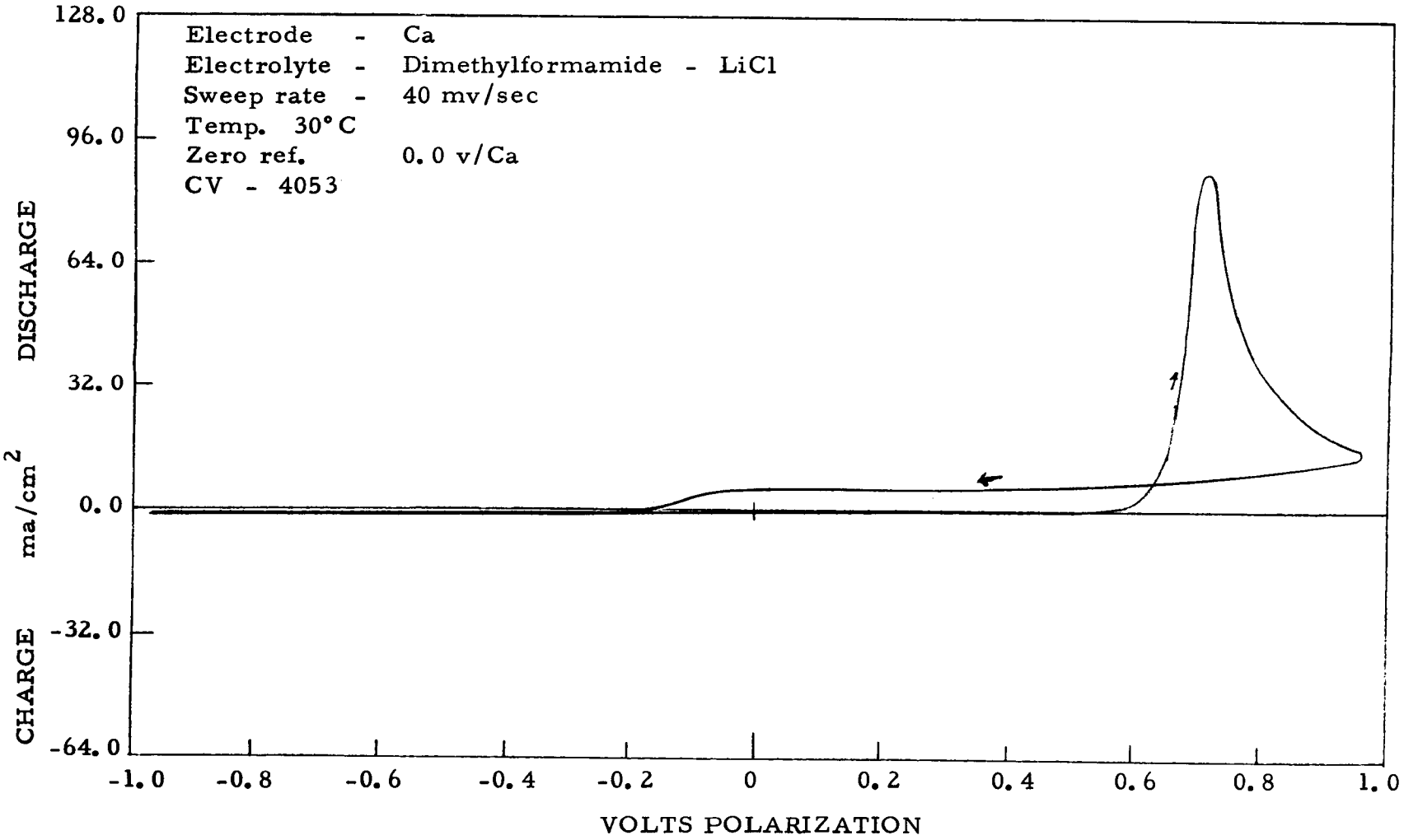
Electrode - Ca
Electrolyte - Dimethylformamide - LiCl
Sweep rate - 40 mv/sec
Temp. 30° C
Zero ref. 0.0 v/Ca
CV - 4053
128.0
96.0
64.0
32.0
0.0
-32.0
-64.0
DISCHARGE
CHARGE
ma/cm2
-1.0
-0.8
-0.6
-0.4
-0.2
0
0.2
0.4
0.6
0.8
1.0
VOLTS POLARIZATION

Figure 7

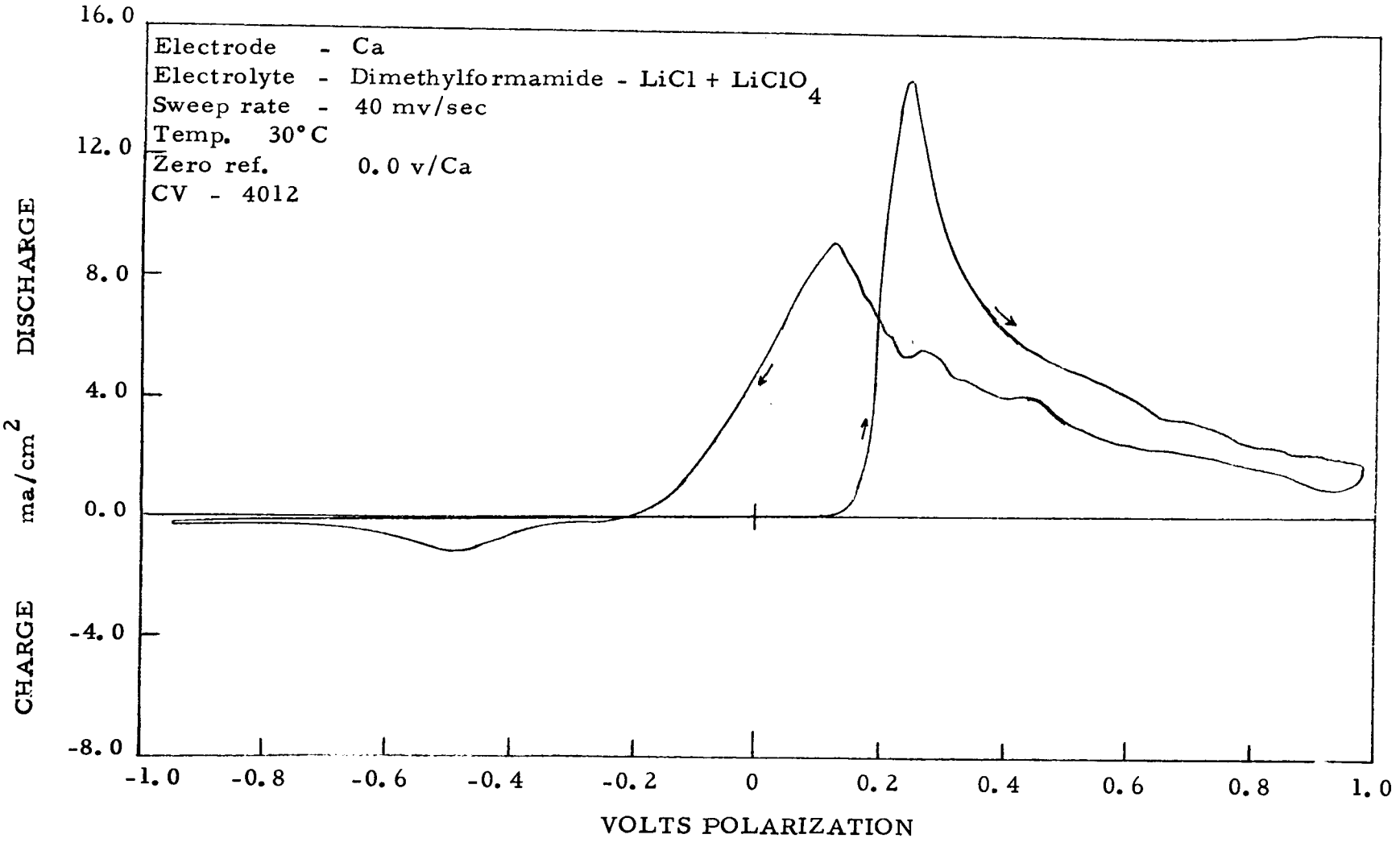
Electrode - Ca
Electrolyte - Dimethylformamide - LiCl + LiClO4
Sweep rate - 40 mv/sec
Temp. 30°C
Zero ref. 0.0 v/Ca
CV - 4012
16.0
12.0
8.0
4.0
0.0
-4.0
-8.0
DISCHARGE
CHARGE
ma/cm2
-1.0
-0.8
-0.6
-0.4
-0.2
0
0.2
0.4
0.6
0.8
1.0
VOLTS POLARIZATION

Figure 8

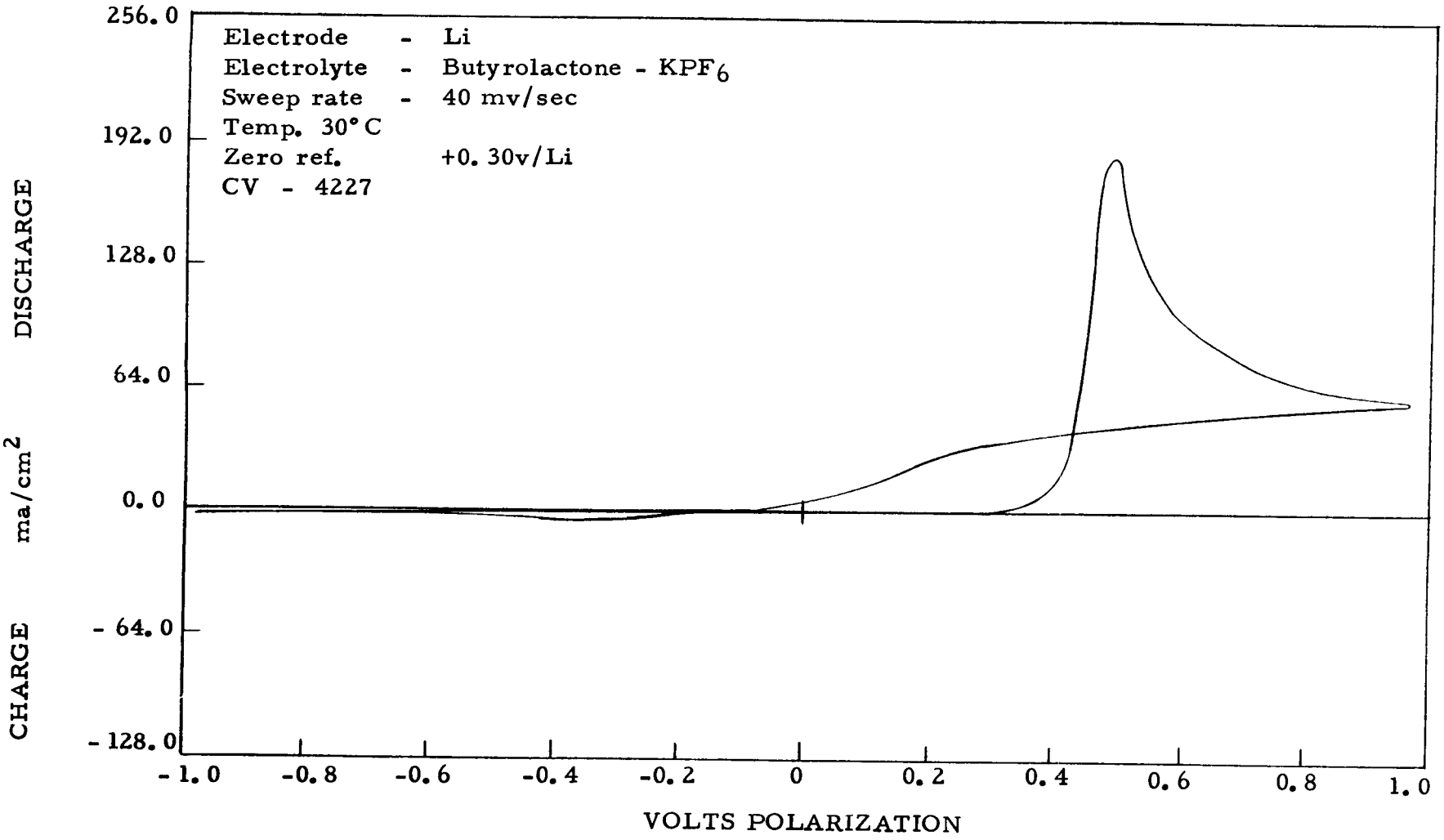
Electrode - Li
Electrolyte - Butyrolactone - KPF_6
Sweep rate - 40 mv/sec
Temp. 30° C
Zero ref. +0.30v/Li
CV - 4227
256.0
192.0
128.0
64.0
0.0
- 64.0
- 128.0
DISCHARGE
CHARGE
ma/cm^2
- 1.0
-0.8
-0.6
-0.4
-0.2
0
0.2
0.4
0.6
0.8
1.0
VOLTS POLARIZATION

Figure 9

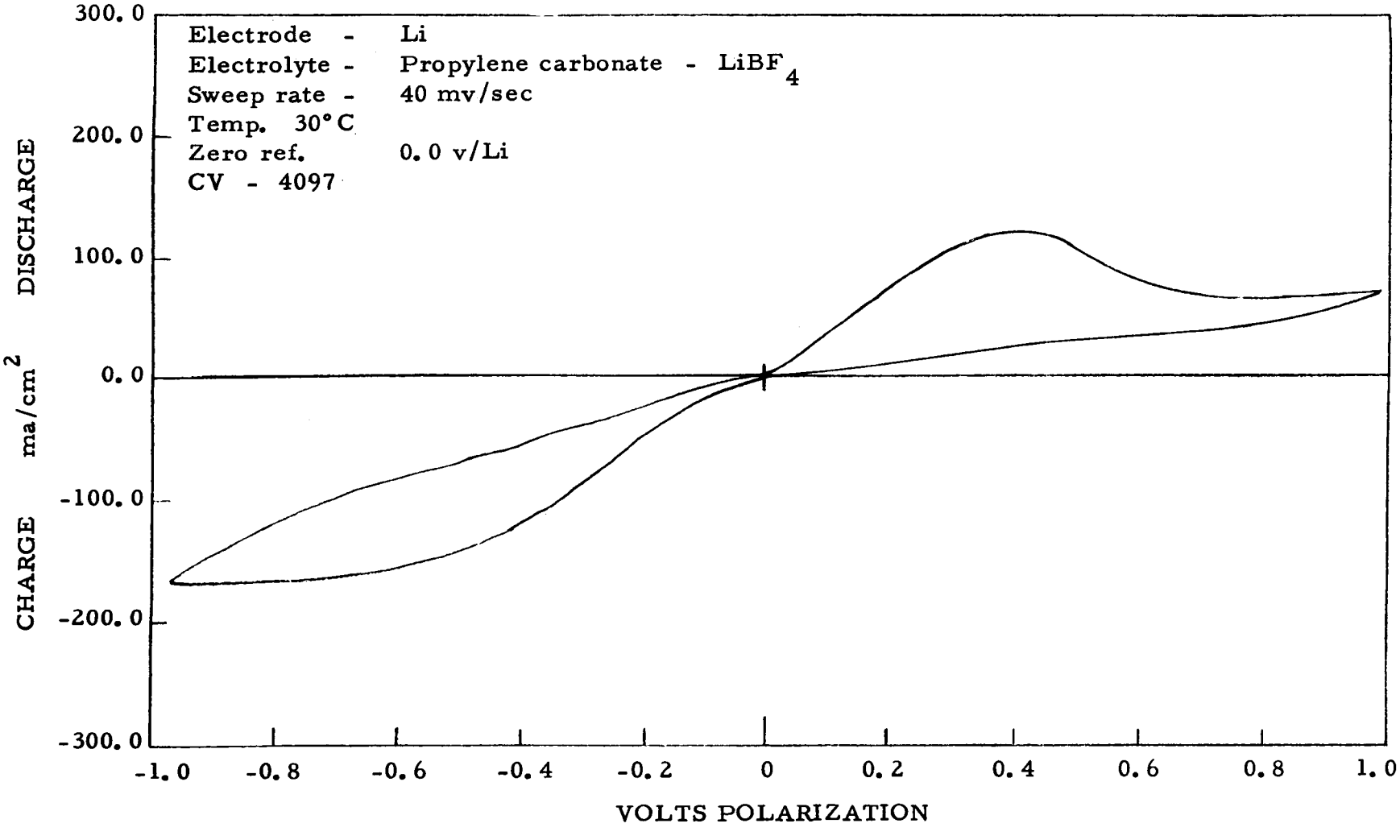
Electrode - Li
Electrolyte - Propylene carbonate - $LiBF_4$
Sweep rate - 40 mv/sec
Temp. 30°C
Zero ref. 0.0 v/Li
CV - 4097
300.0
200.0
100.0
0.0
-100.0
-200.0
-300.0
DISCHARGE
CHARGE
ma/cm^2
-1.0
-0.8
-0.6
-0.4
-0.2
0
0.2
0.4
0.6
0.8
1.0
VOLTS POLARIZATION

Figure 10

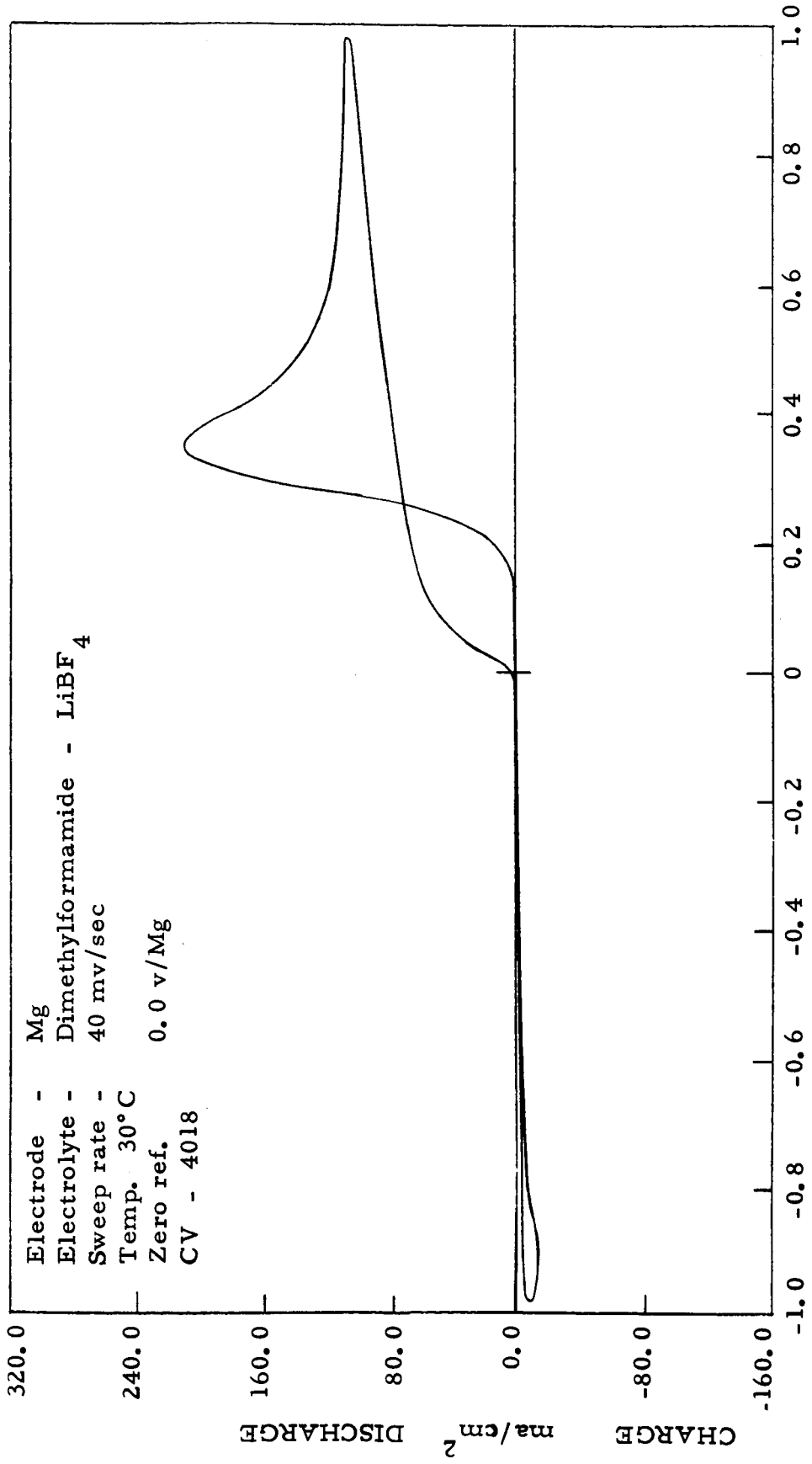
Electrode - Mg
Electrolyte - Dimethylformamide - $LiBF_4$
Sweep rate - 40 mv/sec
Temp. 30°C
Zero ref. 0.0 v/Mg
CV - 4018
320.0
240.0
160.0
80.0
0.0
-80.0
-160.0
CHARGE
DISCHARGE
ma/cm²
-1.0
-0.8
-0.6
-0.4
-0.2
0
0.2
0.4
0.6
0.8
1.0
VOLTS POLARIZATION

Figure 11

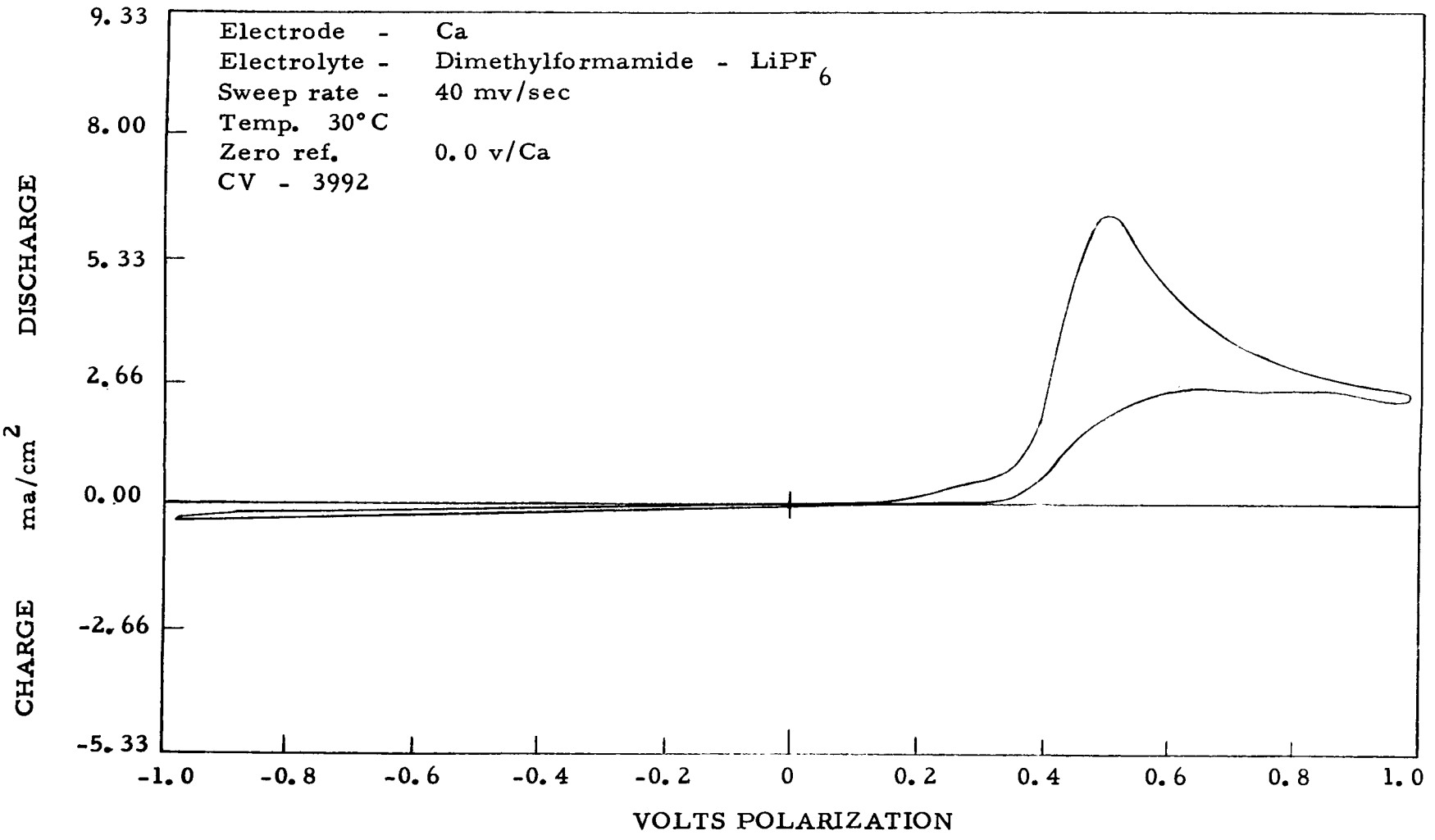
Electrode - Ca
Electrolyte - Dimethylformamide - $LiPF_6$
Sweep rate - 40 mv/sec
Temp. 30°C
Zero ref. 0.0 v/Ca
CV - 3992
9.33
8.00
5.33
2.66
0.00
-2.66
-5.33
DISCHARGE
CHARGE
ma/cm^2
-1.0
-0.8
-0.6
-0.4
-0.2
0
0.2
0.4
0.6
0.8
1.0
VOLTS POLARIZATION

Figure 12

B. Tables of Cyclic Voltammetric Data

Included in this section are tables summarizing the cyclic voltammetric data in terms of peak existence, peak magnitude, and peak displacement, ΔV_p. The peak-to-peak displacement gives a measure of overall electrode reversibility, or in more practical terms, a measure of suitability of the electrochemical system for second battery application.

For comparative purposes, current density magnitude is classified according to very high (more than 300 ma/cm^2), high (100-300 ma/cm^2), medium high (50-100 ma/cm^2), medium low (10-50 ma/cm^2), low (1-10 ma/cm^2), and very low (less than 1 ma/cm^2).

TABLE VIII

SYSTEMS CAUSING VOLTAGE OVERLOAD OF INSTRUMENTATION

System	CV	Max. Anod. C. D. ma/cm^2	Max. Cath. C. D. ma/cm^2
Li/PC-$LiPF_6$	4145	350	800

PC - Propylene carbonate

TABLE IX

PEAK CURRENT DENSITY RANGE

System	CV	Anodic	Cathodic
Li/BL-$LiClO_4$	4135	high	high
Li-BL-$AlCl_3$	4162	high	high
Li/BL-$AlCl_3$ + LiCl	4147	low	med high
Li/DMF-$LiClO_4$	4109	high	med low
Li/DMF-$LiPF_6$	4112	high	high
Li/DMF-$LiBF_4$	4131	very high	med high
Li/PC-$LiClO_4$	4103	med low	med low
Li/PC-$AlCl_3$ + LiCl	4212	med low	low
Li/PC-$MgCl_2$	4152	med low	med low
Li/PC-$LiBF_4$	4097	high	high
Mg/DMF-$LiPF_6$	4013	med high	med low
Ca/AN-$AlCl_3$	4092	high	low
Ca/AN-$AlCl_3$ + LiCl	4087	very high	med low
Ca/DMF-LiCl + $LiClO_4$	4012	med low	very low

AN - Acetonitrile
BL - Butyrolactone
DMF - Dimethylformamide
PC - Propylene carbonate

TABLE X

VOLTAGE SEPARATING ANODIC AND CATHODIC PEAKS

System	CV	ΔV_p
Li/BL-$AlCl_3$	4162	1.6
Li/BL-$LiClO_4$	4135	1.8
Li/DMF-$LiClO_4$	4109	0.6
Li/DMF-$LiBF_4$	4131	1.0
Li/DMF-$LiPF_6$	4112	1.0
Li/PC-$AlCl_3$ + LiCl	4212	0.4
Li/PC-$MgCl_2$	4152	1.3
Mg/DMF-$LiPF_6$	4013	1.6
Ca/AN-$AlCl_3$	4092	0.6
Ca/AN-$AlCl_3$ + LiCl	4087	1.2
Ca/DMF-LiCl + $LiClO_4$	4012	0.7

AN - Acetonitrile
BL - Butyrolactone
DMF - Dimethylformamide
PC - Propylene carbonate

TABLE XI

SYSTEMS EXHIBITING ANODIC PEAK ONLY *
CHLORIDE AND PERCHLORATE ELECTROLYTES

System	CV	Anodic Peak Current Density
$Mg/AN-LiClO_4$	3509	very high
$Mg/AN-Mg(ClO_4)_2$	3489	high
$Mg/AN-AlCl_3$	3514	high (a)
$Mg/AN-AlCl_3 + LiCl$	3529	high (a)
$Mg/BL-LiClO_4$	4172	med low
$Mg/BL-AlCl_3$	4023	high
$Mg/BL-AlCl_3 + LiCl$	4048	high
$Mg/DMF-LiClO_4$	3465	high
$Mg/DMF-Mg(ClO_4)_2$	3459	med low
$Mg/DMF-LiCl$	3472	high
$Mg/DMF-LiCl + LiClO_4$	4205	med high
$Mg/DMF-MgCl_2$	3494	high (a)
$Mg/PC-AlCl_3 + LiCl$	3483	high
$Mg/PC-MgCl_2$	4180	very low
$Ca/AN-LiClO_4$	4185	low
$Ca/BL-AlCl_3$	3982	med low
$Ca/BL-AlCl_3 + LiCl$	3977	med low
$Ca/DMF-LiCl$	4053	med high (b)
$Ca/PC-LiClO_4$	4083	very low

* Maximum cathodic current density in very low range (< 1 ma/cm^2) unless otherwise noted.

(a) Low range cathodic (< 10 ma/cm^2)
(b) Medium high range cathodic (50 - 100 ma/cm^2)

AN - Acetonitrile
BL - Butyrolactone
DMF - Dimethylformamide
PC - Propylene carbonate

TABLE XII

SYSTEMS EXHIBITING ANODIC PEAK ONLY *
FLUORIDE ELECTROLYTES

System	CV	Peak Current Density Range
Li/DMF-KPF_6	4117	med high
Li/BL-KPF_6	4227	high (a)
Mg/AN-$LiPF_6$	4192	very high
Mg/AN-KPF_6 + $LiPF_6$	3499	high
Mg/DMF-KPF_6	3477	med low
Mg/DMF-$LiBF_4$	4018	high (a)
Mg/PC-$LiPF_6$	4038	low
Mg/PC-$LiBF_4$	4036	low
Ca/AN-$LiPF_6$ + KPF_6	4066	high (b)
Ca/BL-KPF_6	3987	very low
Ca/DMF-$LiPF_6$	3992	low
Ca/DMF-KPF_6	4058	med high (a)
Ca/PC-$LiPF_6$	4078	low (a)
Ca/PC-KPF_6	4076	low

* Maximum cathodic current density in very low range (< 1 ma/cm^2) unless otherwise noted.

(a) Low range cathodic (< 10 ma/cm^2)
(b) Medium low range cathodic (10 - 50 ma/cm^2)

AN - Acetonitrile
BL - Butyrolactone
DMF - Dimethylformamide
PC - Propylene carbonate

TABLE XIII

SYSTEMS EXHIBITING CATHODIC PEAK ONLY

System	CV	Peak Current Density Range
Li/PC-KPF_6	4157	low (a)
Li/PC-$Mg(ClO_4)_2$	4197	low (b)

(a) Maximum anodic current in low range (1 - 10 ma/cm^2)

(b) Maximum anodic current in medium low range (10 - 50 ma/cm^2)

PC - Propylene carbonate

TABLE XIV

SYSTEMS EXHIBITING NO PEAKS *

System	CV	
Li/DMF-LiCl	4122	
Li/DMF-LiCl + $LiClO_4$	4127	
Mg/AN-KPF_6	3519	(a)
Mg/AN-$LiBF_4$	4226	(a)
Mg/BL-KPF_6	4028	
Mg/PC-$LiClO_4$	4046	
Mg/PC-KPF_6	3504	
Ca/AN-$LiPF_6$	4071	(a)
Ca/AN-$LiBF_4$	4223	
Ca/BL-$LiClO_4$	4190	
Ca/DMF-$LiClO_4$	4001	
Ca/DMF-$LiBF_4$	3996	(a)
Ca/PC-$AlCl_3$ + LiCl	4217	
Ca/PC-$LiBF_4$	4238	(b)

* Maximum current density in very low range (< 1 ma/cm^2) unless otherwise noted.

(a) Medium low range (10 - 50 ma/cm^2)
(b) High range (> 300 ma/cm^2)

AN - Acetonitrile
BL - Butyrolactone
DMF - Dimethylformamide
PC - Propylene carbonate

C. Choice of Negative-Electrolyte Systems

As detailed in the Seventh Quarterly report, (Ref. 1) recommendation of systems was based on peak height and shape (using Sweep Index as a relative figure of merit) as well as peak displacement. The nature of the sweep curves obtained for the negative systems does not allow a weighting and elimination procedure in terms of peak height, sweep index, and peak displacement. For convenience, however, data from the preceding tables are rearranged to summarize the results for the negative-electrolyte systems, which are discussed in terms of the electrode.

1. Lithium Systems

Table XV summarizes the lithium data. Lithium was not screened in acetonitrile because of known lack of compatibility in this solvent. There was visual evidence of lithium decomposition in dimethylformamide on both the working and reference electrodes. Chemical and electrochemical reactivity appear to be related with each other, and chloride ion appears to inhibit the reactivity of lithium in dimethylformamide. These observations are tabulated in Table XVI.

Elimination of lithium systems in dimethylformamide is recommended at this time. Additional efforts with lithium in dimethylformamide electrolytes should investigate the use of passivating agents such as calcium, magnesium, and quaternary ammonium chloride salt additives.

Table XVII contains a listing of the coulombic densities of the lithium systems in butyrolactone and propylene carbonate. The coulombic density represents the total integrated current density for either the anodic (discharge) or cathodic (charge) portions of the cycle. The values are listed in order of decreasing charge coulombic density. The charge or cathodic coulombic density corresponds to the sum total of the electrochemical reduction taking place at the working electrode during the cycle. This

includes species produced during the anodic (discharge) cycle and remaining at or in the vicinity of the working electrode, as well as species diffusing, or carried by convection, to this electrode from the bulk solution.

Calculation of the contribution to the cathodic coulombic density, due to a 1 molar concentration of electrode active species in solution during the cathodic half cycle (50 seconds), is of the order of 5 coulombs/cm^2, assuming ideal conditions and no convection. As seen from the Table, this value is approached by only a few systems, and generally only by those containing lithium salts. The lowest values occur for magnesium and potassium salts. It is significant that in all cases where lithium electrolytes are used, the cathodic coulombic density is always greater than the anodic value. Similarly, in the absence of lithium salts, the discharge coulombic density is greater than the cathodic value. These results reflect in part, the rechargeability of the system. Propylene carbonate - $LiPF_6$ gives the highest in both the charge and discharge coulombic density, with propylene carbonate - KPF_6 giving the lowest.

TABLE XV

LITHIUM SYSTEMS

System	CV	Maximum Current Density Anodic ma/cm^2	Cathodic ma/cm^2
Li/PC-$LiPF_6$	4145 vo	very high	very high
Li/DMF-$LiBF_4$	4131	very high	med high
Li/BL-KPF_6	4227 a	high	low
Li/BL-$LiClO_4$	4135	high	high
Li/BL-$AlCl_3$	4162	high	high
Li/DMF-$LiClO_4$	4109	high	med low
Li/DMF-$LiPF_6$	4112	high	high
Li/PC-$LiBF_4$	4097	high	high
Li/DMF-KPF_6	4117 a	med high	very low
Li/PC-$Mg(ClO_4)_2$	4197 c	med low	low
Li/PC-$LiClO_4$	4103	med low	med low
Li/PC-$AlCl_3$ + LiCl	4212	med low	low
Li/PC-$MgCl_2$	4152	med low	med low
Li/PC-KPF_6	4157 c	low	low
Li/BL-$AlCl_3$ + LiCl	4147	low	med high
Li/DMF-LiCl + $LiClO_4$	4127 np	very low	low
Li/DMF-LiCl	4122 np	very low	very low

vo - Voltage overload
a - Anodic peak only
c - Cathodic peak only
np - No peaks

BL - Butyrolactone
DMF - Dimethylformamide
PC - Propylene carbonate

TABLE XVI

LITHIUM/DIMETHYLFORMAMIDE SYSTEMS

Solute	CV	Max. Anod. C. D. ma/cm^2	Max. Cath. C. D. ma/cm^2	Observations
$LiBF_4$	4131	very high	high	gassing
$LiClO_4$	4109	very high	med low	white precipitate
$LiPF_6$	4112	high	high	dark orange solution
KPF_6	4117	med high	low	brown-cloudy solution
LiCl + $LiClO_4$	4127	med low	very low	clear solution
LiCl	4122	very low	very low	light yellow solution

TABLE XVII

LITHIUM SYSTEMS

System	CV	Coulombic Density *	
		Anodic coul/cm^2	Cathodic coul/cm^2
Li/BL-$LiClO_4$	4135	2.5	3.3
Li/BL-$AlCl_3$	4162	2.8	2.1
Li/BL-$AlCl_3$ + LiCl	4147	0.35	0.98
Li/BL-KPF_6	4227	2.4	0.07
Li/PC-$LiPF_6$	4145	>5 (a)	5
Li/PC-$LiBF_4$	4097	2.7	4.5
Li/PC-$LiClO_4$	4103	0.76	0.97
Li/PC-$AlCl_3$ + LiCl	4212	0.38	0.42
Li/PC-$MgCl_2$	4152	0.70	0.39
Li/PC-$Mg(ClO_4)_2$	4197	0.33	0.09
Li/PC-KPF_6	4157	0.06	0.05

* - In order of decreasing cathodic coulombic density

(a) - Data approximate due to marginal voltage overload

BL - Butyrolactone
PC - Propylene carbonate

2. Magnesium Systems

Table XVIII represents a list of all magnesium systems screened. The latter show generally high anodic activity but very little or no cathodic activity. The anodic activity was generally higher in acetonitrile and dimethylformamide solutions than in butyrolactone and propylene carbonate solutions. Electrolytes containing potassium, lithium, aluminum and magnesium, all behaved similarly in this respect. Only three systems, DMF-$LiPF_6$, DMF-$LiBF_4$, and AN-$LiBF_4$, show maximum cathodic current density greater than 10 ma/cm^2, and this activity occurs at about 1 volt negative to the open circuit voltage at potentials near the lithium ion reduction.

In view of the above, none of the magnesium systems screened can be recommended for secondary battery application. However, further molecular level studies are recommended, using complex metal fluoride and fluoride salts of magnesium and tetraalkylammonium cations.

TABLE XVIII

MAGNESIUM SYSTEMS

System	CV	Maximum Current Density Anodic ma/cm^2	Cathodic ma/cm^2
Mg/AN-$LiPF_6$	4192 a	very high	very low
Mg/AN-$LiClO_4$	4169 a	very high	very low
Mg/AN-KPF_6 + $LiPF_6$	3499 a	high	very low
Mg/DMF-$LiBF_4$	4018 a	high	med low
Mg/AN-$Mg(ClO_4)_2$	3489 a	high	very low
Mg/AN-$AlCl_3$	3514 a	high	very low
Mg/AN-$AlCl_3$ + LiCl	3529 a	high	low
Mg/BL-$AlCl_3$	4023 a	high	very low
Mg/BL-$AlCl_3$ + LiCl	4048 a	high	very low
Mg/DMF-$LiClO_4$	3465 a	high (d)	very low
Mg/DMF-LiCl	3472 a	high	very low
Mg/DMF-$MgCl_2$	3494 a	high	very low
Mg/PC-$AlCl_3$ + LiCl	3483 a	high	very low
Mg/DMF-$LiPF_6$	4013	med high	med low
Mg/DMF-LiCl + $LiClO_4$	4205 a	med high	very low
Mg/DMF-KPF_6	3477 a	med low	very low
Mg/BL-$LiClO_4$	4172 a	med low	very low
Mg/DMF-$Mg(ClO_4)_2$	3459 a	med low (d)	very low
Mg/AN-KPF_6	3519 np	med low	very low
Mg/PC-$LiPF_6$	4038 a	low	very low
Mg/PC-$LiBF_4$	4036 a	low	very low
Mg/AN-$LiBF_4$	4226 np	low	med low
Mg/BL-KPF_6	4028 np	very low	very low
Mg/PC-$LiClO_4$	4046 np	very low	very low
Mg/PC-KPF_6	3504 np	very low	very low
Mg/PC-$MgCl_2$	4180 a	very low	very low

(d) - Electrode area reduced more than 50% by dissolution

a - Anodic peak only
np - No peaks

AN - Acetonitrile
BL - Butyrolactone
DMF - Dimethylformamide
PC - Propylene carbonate

3. Calcium Systems

Table XIX represents a list of all calcium systems screened. These systems yield results similar to those obtained with magnesium in that relatively little cathodic activity is obtained. Generally greater anodic activity is observed in acetonitrile and dimethylformamide solutions and less in butyrolactone and propylene carbonate solutions. An exception occurs with the system Ca/PC-$LiBF_4$ (CV-4238), but it is uncertain that the cathodic reaction is due to calcium or lithium ions from the electrolyte, because of the close proximity of the electrode potentials for both metals. The cathodic peak current density (285 ma/cm^2) is about twice what would be expected for lithium ions for the 0.5 m $LiBF_4$ electrolyte. However, the curve is recorded after ten sweep cycles, and by this time, changes in concentration at the electrode surface as well as the presence of convection currents, can account for the large cathodic current. In addition, the cathodic coulombic density is several times that for the anodic peak, again suggesting the reduction of species from solution.

The low cathodic activity for the calcium systems does not permit their recommendation for secondary battery application. However, in view of the favorable discharge (anodic) currents, it is recommended that additional screening of calcium be carried out in calcium and tetralkylammonium salt electrolytes.

TABLE XIX

CALCIUM SYSTEMS

System	CV		Maximum Current Density Anodic ma/cm^2	Cathodic ma/cm^2
Ca/AN-$AlCl_3$ + LiCl	4087		very high	med low
Ca/AN-$AlCl_3$	4092		high	low
Ca/AN-$LiPF_6$ + KPF_6	4066	a	high	low
Ca/AN-$LiPF_6$	4071	np	med high	med low
Ca/DMF-KPF_6	4058	a	med high	low
Ca/DMF-LiCl	4053	a	med high	low
Ca/PC-$LiBF_4$	4238	np	med low	high
Ca/DMF-LiCl + $LiClO_4$	4012		med low	very low
Ca/BL-$AlCl_3$	3982	a	med low	very low
Ca/BL-$AlCl_3$ + LiCl	3977	a	med low	very low
Ca/DMF-$LiPF_6$	3992	a	low	very low
Ca/PC-$LiPF_6$	4078	a	low	low
Ca/PC-KPF_6	4076	a	low	very low
Ca/AN-$LiClO_4$	4185	a	low	very low
Ca/AN-$LiBF_4$	4223	np	very low	very low
Ca/BL-$LiClO_4$	4190	np	very low	very low
Ca/DMF-$LiClO_4$	4001	np	very low	very low
Ca/DMF-$LiBF_4$	3996	np	very low	low
Ca/PC-$AlCl_3$ + LiCl	4217	np	very low	very low
Ca/BL-KPF_6	3987	a	very low	very low
Ca/PC-$LiClO_4$	4083	a	very low	very low

a - Anodic peak only
np - No peaks

AN - Acetonitrile
BL - Butyrolactone
DMF - Dimethylformamide
PC - Propylene carbonate

III. REFERENCES

1. Whittaker Corporation, Narmco R and D Division, Seventh Quarterly Report, NASA Contract 3-8509, NASA CR-72377, February 1968.

DISTRIBUTION LIST

National Aeronautics and Space Admin.
Washington, D. C. 20546
Attn: E. M. Cohn/RNW
A. M. Greg Andrus/PC

National Aeronautics and Space Admin.
Goddard Space Flight Center
Greenbelt, Maryland 20771
Attn: T. Hennigan, Code 716.2
J. Sherfey, Code 735
P. Donnelly, Code 636.2
E. R. Stroup, Code 636.2

National Aeronautics and Space Admin.
Langley Research Center
Instrument Research Division
Hampton, Virginia 23365
Attn: J. L. Patterson, MS 234
M. B. Seyffert, MS 112

National Aeronautics and Space Admin.
Langley Research Center
Hampton, Virginia 23365
Attn: S. T. Peterson
Harry Ricker

National Aeronautics and Space Admin.
Lewis Research Center
21000 Brookpark Road
Cleveland, Ohio 44135
Attn: Library, MS 60-3
N. D. Sanders, MS 302-1
John E. Dilley, MS 500-309
B. Lubarsky, MS 500-201
H. J. Schwartz, MS 500-201
R. B. King, MS 500-201 (2cys.)
V. F. Hlavin, MS 3-14 (Final only)
M. J. Saari, MS 500-202
J. J. Weber, MS 3-19
Report Control, MS 5-5
Dr. J. S. Fordyce, MS 6-1

National Aeronautics and Space Admin.
Scientific and Tech. Information Facility
P. O. Box 33
College Park, Maryland 20740
Attn: Acquisitions Branch (SQT-34054)
(2 cys. + 1 repro.)

National Aeronautics and Space Admin.
George C. Marshall Space Flight Center
Huntsville, Alabama 35812
Attn: Philip Youngblood
R. Boehme, Bldg. 4487.BB,
M-ASTR-EC

National Aeronautics and Space Admin.
Manned Spacecraft Center
Houston, Texas 77058
Attn: W. R. Dusenbury, Propulsion
and Energy Systems
R. Cohen (KS 111)
R. Ferguson (EP-5)
F. E. Eastman (EE-4)

National Aeronautics and Space Admin.
Ames Research Center
Pioneer Project
Moffett Field, California 94035
Attn: J. R. Swain
A. S. Hertzog
J. Rubenzer, Biosatellite Project

Jet Propulsion Laboratory
4800 Oak Grove Drive
Pasadena, California 91103
Attn: A. Uchiyama

U. S. Army Engineer R and D Labs.
Fort Belvoir, Virginia 22060
Attn: Electrical Power Branch
SMOFB-EP

Commanding Officer
U. S. Army Electronics R and D Labs
Fort Monmouth, New Jersey 07703
Attn: Power Sources Div.,
Code SELRA/PS

Research Office
R and D Directorate
Army Weapons Command
Rock Island, Illinois 61201
Attn: G. Riensmith, Chief

U. S. Army Research Office
Box CM, Duke Station
Durham, North Carolina 27706
Attn: Dr. W. Jorgensen

U. S. Army Research Office
Chief, R and D
Department of the Army
3 D 442, The Pentagon
Washington, D. C. 20546

Harry Diamond Laboratories
Room 300, Bldg. 92
Conn. Ave and Van Ness St., NW
Washington, D. C. 20438
Attn: N. Kaplan

Army Materiel Command
Research Division
AMCRD-RSCM-T-7
Washington, D. C. 20315
Attn: J. W. Crellin

Army Materiel Command
Development Division
AMCRO-DE-MO-P
Washington, D. C. 20315
Attn: M. D. Aiken

U. S. Army TRECOM
Fort Eustis, Virginia 23604
Attn: Dr. R. L. Echols (SMOFE-PSG)
L. M. Bartone (SMOFE-ASE)

U. S. Army R and L Liaison Group
(9851 DV) APO 757
New York, New York 10004
Attn: B. R. Stein

Office of Naval Research
Department of the Navy
Washington, D. C. 20360
Attn: Head, Power Branch, Code 429
H. W. Fox, Code 425

Naval Research Laboratory
Washington, D. C. 20390
Attn: Dr. J. C. White, Code 6160

U. S. Navy
Marine Engineering Laboratory
Annapolis, Maryland 21402
Attn: J. H. Harrison

Bureau of Naval Weapons
Department of the Navy
Washington, D. C. 20360
Attn: W. T. Beatson, Code RAAE-52
M. Knight, Code RAAE-50

Naval Ammunition Depot
Crane, Indiana 47522
Attn: E. Bruess
H. Schultz

Naval Ordnance Laboratory
Department of the Navy
Corona, California 91720
Attn: W. C. Spindler, Code 441

Army Reactors, DRD
U. S. Atomic Energy Commission
Washington, D. C. 20545
Attn: D. B. Hoatson

Naval Ordnance Laboratory
Department of the Navy
Silver Springs, Maryland 20900
Attn: P. B. Cole, Code WB

Bureau of Ships
Department of the Navy
Washington, D. C. 20360
Attn: B. B. Rosenbaum, Code 340
C. F. Viglotti, Code 660

Space Systems Division
Los Angeles AF Station
Los Angeles, California 90045
Attn: SSSD

Air Force Cambridge Research Lab.(CRFE)
L. G. Hanscom Field
Bedford, Massachusetts 01731
Attn: Dr. Richard Payne

Flight Vehicle Power Branch
Aero Propulsion Laboratory
Wright-Patterson AFB, Ohio 45433
Attn: J. E. Cooper
Dr. J. J. Lander

Headquarters, USAF (AFRDR-AS)
Washington, D. C. 20546
Attn: Maj. G. Starkey
Lt. Col. W. G. Alexander

Rome Air Development Center, ESD
Griffis AF Base, New York 13442
Attn: F. J. Mollura (RASSM)

National Bureau of Standards
Washington, D. C. 20234
Attn: Dr. W. J. Hamer

Office DDR and E, USE and BSS
The Pentagon
Washington, D. C. 20310
Attn: G. B. Wareham

Institute for Defense Analyses
R and E Support Division
400 Army-Navy Drive
Arlington, Virginia 22022
Attn: R. Hamilton
Dr. G. C. Szego

U. S. Atomic Energy Commission
Auxiliary Power Branch (SNAP)
Division of Reactor Development
Washington, D. C. 20545
Attn: Lt. Col. G. H. Ogburn, Jr.

U. S. Atomic Energy Commission
Advanced Space Reactor Branch
Division of Reactor Development
Washington, D. C. 20545
Attn: Lt. Col. J. H. Anderson

Office of Technical Services
Department of Commerce
Washington, D. C. 20009

Aerojet-General Corporation
Von Karman Center
Building 312/Dept. 3111
Azusa, California 91703

Aeronutronic Division
Philco Corporation
Ford Road
Newport Beach, California 92660

Aerospace Corporation
P. O. Box 95085
Los Angeles, California 90045
Attn: Library

Burgess Battery Company
Foot of Exchange Street
Freeport, Illinois 61032
Attn: Dr. Howard J. Strauss

Aerospace Corporation
Systems Design Division
2350 East El Segundo Boulevard
El Segundo, California 90246
Attn: John G. Krisilas

Allis-Chalmers Manufacturing Company
Research Division Library
P. O. Box 512
Milwaukee, Wisconsin 53201

American University
Massachusetts and Nebraska Avenues NW
Washington, D. C. 20016
Attn: Dr. R. T. Foley, Chemistry Dept.

Arthur D. Little, Incorporated
Acorn Park
Cambridge, Massachusetts 02140
Attn: Dr. Ellery W. Stone

Atomics International Division
North American Aviation, Incorporated
8900 DeSoto Avenue
Canoga Park, California 91304
Attn: Dr. H. L. Recht

Battelle Memorial Institute
505 King Avenue
Columbus, Ohio 43201
Attn: Dr. C. L. Faust

Bell Laboratories
Murray Hill, New Jersey 07971
Attn: U. B. Thomas

The Boeing Company
P. O. Box 3707
Seattle, Washington 98124

Borden Chemical Company
Central Research Laboratory
P. O. Box 9524
Philadelphia, Pennsylvania 19124

C and D Batteries
Division of Electric Autolite Company
Conshohocken, Pennsylvania 19428
Attn: Dr. Eugene Willihnganz

Calvin College
Grand Rapids, Michigan 49506
Attn: Prof. T. P. Dirkse

Catalyst Research Corporation
6101 Falls Road
Baltimore, Maryland 21209
Attn: J. P. Wooley

ChemCell, Incorporated
150 Dey Road
Wayne, New Jersey 07470
Attn: Peter D. Richman

Delco-Remy Division
General Motors Corporation
2401 Columbus Avenue
Anderson, Indiana 46011
Attn: John Keralla

Douglas Aircraft Company, Incorporated
Astropower Laboratory
2121 Campus Drive
Newport Beach, California 92663

Dynatech Corporation
17 Tudor Street
Cambridge, Massachusetts 02138
Attn: R. L. Wentworth

Eagle-Pitcher Company
P. O. Box 47
Joplin, Missouri 64802
Attn: E. M. Morse

General Electric Company
Battery Products Section
P. O. Box 114
Gainesville, Florida 32601
Attn: Dr. R. L. Hadley

Elgin National Watch Company
107 National Street
Elgin, Illinois 60120
Attn: T. Boswell

Electric Storage Battery Company
Missile Battery Division
2510 Louisburg Road
Raleigh, North Carolina 27604
Attn: A. Chreitzberg

Electric Storage Battery Company
Carl F. Norberg Research Center
Wardley, Pennsylvania 19068
Attn: Dr. R. A. Schaefer

Electrochimica Corporation
1140 O'Brien Drive
Menlo Park, California 94025
Attn: Dr. Morris Eisenberg

Electro-Optical Systems, Incorporated
300 North Halstead
Pasadena, California 91107
Attn: E. Findl

Emhart Manufacturing Company
Box 1620
Hartford, Connecticut 06101
Attn: Dr. W. P. Cadogan

Englehard Industries, Incorporated
497 Delancy Street
Newark, New Jersey 07105
Attn: Dr. J. G. Cohn

Dr. Arthur Fleischer
466 South Center Street
Orange, New Jersey 07050

Grumman Aircraft
CPGS Plant 35
Beth Page, Long Island, New York 11101
Attn: Bruce Clark

General Electric Company
Research and Development Center
Schenectady, New York 12301
Attn: Dr. H. Liebhafsky
Dr. R. C. Osthoff, Bldg. 37.

General Telephone and Electronics Labs.
Bayside, New York 11352
Attn: Library

Globe-Union, Incorporated
900 East Keefe Avenue
Milwaukee, Wisconsin 53201
Attn: Dr. Clarence K. Morehouse

Gould-National Batteries, Incorporated
Engineering and Research Center
2630 University Avenue, SE
Minneapolis, Minnesota 55418
Attn: D. L. Douglas

Gulton Industries
Alkaline Battery Division
212 Durham Avenue
Metuchen, New Jersey 08840
Attn: Dr. Robert Shair

Leesona Moos Laboratories
Lake Success Park, Community Drive
Great Neck, New York 11021
Attn: Dr. H. Oswin

Livingston Electronic Corporation
Route 309
Montgomeryville, Pennsylvania 18936
Attn: William F. Meyers

Hughes Aircraft Corporation
Centinela Avenue and Teale Street
Culver City, California 90230
Attn: T. V. Carvey

Hughes Aircraft Corporation
Building 366, MS 524
El Segundo, California 90245
Attn: R. B. Robinson

Hughes Research Labs. Corp.
2011 Malibu Canyon Road
Mailbu, California 90265
Attn: T. M. Hahn

ITT Federal Laboratories
500 Washington Avenue
Nutley, New Jersey 07110
Attn: Dr. P. E. Lightly

IIT Research Institute
10 West 35 Street
Chicago, Illinois 60616
Attn: Dr. H. T. Francis

Idaho State University
Department of Chemistry
Pocatello, Idaho 83201
Attn: Dr. G. Myron Arcand

Institute of Gas Technology
State and 34 Street
Chicago, Illinois 60616
Attn: B. S. Baker

John Hopkins University
Applied Physics Laboratory
8621 Georgia Avenue
Silver Springs, Maryland 20910

Lockheed Missiles and Space Co.
3251 Hanover Street
Palo Alto, California 94304
Attn: Library
Dr. G. B. Adams

Lockheed Missiles and Space Co.
Department 52-30
Palo Alto, California 94304
Attn: J. E. Chilton

Lockheed Missiles and Space Co.
Department 65-82
Palo Alto, California 94304
Attn: Larry E. Nelson

P. R. Mallory and Co., Inc.
Technical Services Laboratory
Indianapolis, Indiana 46206
Attn: A. S. Doty

P. R. Mallory and Co., Inc.
3029 East Washington Street
Indianapolis, Indiana 46206
Attn: Library

Marquardt Corporation
16555 Saticoy Street
Van Nuys, California 91406
Attn: Dr. H. G. Krull

Philco Corporation
Division of Ford Motor Company
Blue Bell, Pennsylvania 19422
Attn: Dr. Phillip Cholet

Radiation Applications, Inc.,
36-40 37th Street
Long Island City, New York 11101

Material Research Corporation
Orangeburg, New York 10962
Attn: V. E. Adler

Melpar
Technical Information Center
3000 Arlington Boulevard
Falls Church, Virginia 22046

Metals and Control Division
Texas Instruments, Inc.
34 Forest Street
Attleboro, Massachusetts 02703
Attn: Dr. E. M. Jost

Midwest Research Institute
425 Volker Boulevard
Kansas City, Missouri 64110
Attn: Dr. B. W. Beadle

Monsanto Research Corporation
Everett, Massachusetts 02149
Attn: Dr. J. O. Smith

North American Aviation, Inc.
Rocketdyne Division
6633 Canoga Avenue
Canoga Park, California 91303
Attn: Library

Ozark Mahoning Company
1870 S. Boulder Avenue
Tulsa, Oklahoma 74119
Attn: Dr. James Beal

Power Information Center
University of Pennsylvania
3401 Market Street, Room 2107
Philadelphia, Pennsylvania 19104

Tyco Laboratories, Inc.
Bear Hill
Hickory Drive
Waltham, Massachusetts 02154
Attn: W. W. Burnett

Radio Corporation of America
Astro Division
Highstown, New Jersey 08520
Attn: Seymour Winkler

Radio Corporation of America
P. O. Box 800
Princeton, New Jersey 08540
Attn: L. Schulman

Sandia Corporation
Box 5800
Albuquerque, New Mexico 87115
Attn: Technical Library (2 copies)

Sonotone Corporation
Saw Mill River Road
Elmsford, New York 10523
Attn: A. Mundel

Texas Instruments, Inc.
13500 North Central Expressway
Dallas, Texas 75222
Attn: Dr. Isaac Trachtenberg

Thomas A. Edison Research Lab.
McGraw Edison Company
Watchung Avenue
West Orange, New Jersey 07052
Attn: Dr. P. F. Grieger

TRW Incorporated
TRW Systems Group
One Space Park
Redondo Beach, California 90278
Attn: Dr. A. Krausz, Bldg. 60, Rm 1470

TRW Incorporated
23555 Euclid Avenue
Cleveland, Ohio 44117
Attn: Librarian

Union Carbide Corporation
Development Laboratory Library
P. O. Box 6056
Cleveland, Ohio 44101

Union Carbide Corporation
Parma Research Center
P. O. Box 6116
Cleveland, Ohio 44101
Attn: Library

University of California
Space Science Laboratory
Berkeley, California 94720
Attn: Dr. C. W. Tobias

University of Pennsylvania
Electrochemistry Laboratory
Philadelphia, Pennsylvania 19104
Attn: Prof. J. O'M Brockris

University of Toledo
Toledo, Ohio 43606
Attn: Dr. Albertine Krohn

Western Electric Company
Suite 802, RCA Building
Washington, D. C. 20006
Attn: R. T. Fiske

Westinghouse Electric Corporation
Research and Development Center
Churchill Borough
Pittsburgh, Pennsylvania 15235
Attn: Dr. A. Langer

Whittaker Corporation
Power Sources Division
3850 Olive Street
Denver, Colorado 80237
Attn: J. W. Reiter
Dr. E. Doucette

Whittaker Corporation
Narmco R and D Division
12032 Vose Street
North Hollywood, California 91605
Attn: Dr. M. Shaw

Yardney Electric Corporation
40-50 Leonard Street
New York, New York 10013
Attn: Dr. George Dalin